Strong ground acceleration seismic hazard in Greece and neighboring regions

Paul W. Burton[a,*], Yebang Xu[a], G.-Akis Tselentis[b], Ethimios Sokos[b], Willy Aspinall[c]

[a]*School of Environmental Sciences, University of East Anglia, Norwich NR4 7TJ, UK*
[b]*Seismology Laboratory, University of Patras, Rio 261 10 Greece*
[c]*Aspinall and Associates, 5 Woodside Close, Beaconsfield HP9 1JQ, UK*

Abstract

In an early paper [Tectonophysics 117 (1985) 259] seismic hazard in Greece was analyzed using a relatively homogeneous earthquake catalogue spanning 1900–1978 and a strong motion attenuation relationship adapted to use in Greece. Improved seismic hazard analyses are obtained here using Gumbel's asymptotic extreme value distribution applied to peak horizontal ground acceleration occurrence, but now taking into account the increased length and quality of earthquake catalogue data spanning 1900–1999 and the burgeoning information on earthquake strong motion data and attenuation relationships appropriate for Europe and, explicitly, Greece. Seismic acceleration hazard results tabulated for six cities reveal (e.g. using arbitrarily the 50-year p.g.a. with 90% probability of not being exceeded) changes of about 10% in the new calculated values: two cities show an increase and four a decrease. These are relatively small and reassuring adjustments.

Inspection of the available attenuation relationships leads to a preference for the models of Theodulidis and Papazachos, particularly with the model modification to produce a 'stiff soil' site relationship, as these relationships explicitly exploit the Greek strong motion database. Isoacceleration maps are produced for Greece as a whole from each attenuation relationship inspected. The final set of maps based on the Theodulidis and Papazachos models provide a foundation for comparison with the Seismic Hazard Zones adopted in the New Greek Seismic Code where scope can be found to modify zone shape and the level at which p.g.a.s are set. It should be noted that the generation of the present isoacceleration maps is based on a seismogenic zone-free methodology, independent of any Euclidean zoning assumptions.
© 2003 Elsevier Science Ltd. All rights reserved.

Keywords: Seismic hazard; Strong ground motion; Peak ground acceleration; Greece

1. Introduction

The development of seismic hazard assessment in Greece has a substantial history and has produced considerable progress and innovation. Amongst these developments are studies involving maximum seismic intensity [18,35], peak ground acceleration (p.g.a.) [27,35], simulation of ground motion and design earthquakes [29,30,32,46], suitable strong motion attenuation relations for p.g.a. and response spectra [27,43,47], and site effects [46]. Papaioannou and Papazachos [34] assessed time-independent and time-dependent hazard for 144 regional sites in Greece in terms of the expected macroseismic intensities at these sites based on seismogenic zones.

Gumbel's asymptotic distributions of extreme values [20] have long provided important tools for seismic hazard estimation [11,12,40,50,52 and references therein]. Makropoulos and Burton [26] applied the Gumbel III distribution to seismicity in Greece to evaluate seismic hazard in terms of magnitude recurrence; they also analyzed seismic strain energy accumulation and its release. The Gumbel I distribution was used by Makropoulos and Burton ([27]: referred to as MB) to analyze seismic hazard for Greece in terms of p.g.a.—this analysis also proposed and adopted the MB average formula (see Eq. (4) later) to estimate the attenuation of p.g.a. as a function of distance in Greece. The results of this 1985 paper included p.g.a. hazard estimated at each of six major Greek cities, and the same detailed p.g.a. hazard evaluation procedure is also applied on a matrix of points to the whole area of Greece producing isoacceleration maps. This method has also been used elsewhere in the world [21].

More than 15 years have passed since the work of Makropoulos and Burton [27] and we find at least six reasons why it is important to reassess strong ground acceleration seismic hazard in Greece.

Firstly, more events have been recorded, the quality of the earthquake catalogue has been improved greatly, and so it is important to use the new data to reexamine the acceleration seismic hazard estimations made by Makropoulos and Burton [27]. In conjunction with this need is the recognition that statistical seismic hazard analysis provides a snapshot of seismic hazard built on the previous earthquake history and a tacit recognition that the assumption of stationarity in the process is imperfect. 'Rogue' or 'unexpected' earthquakes [11] do occur and the Athens earthquake of 1999 September 7 (5.9 M_S) provides a salutary reminder of this. Statistical seismic hazard represents past experience and must be updated from time-to-time to provide improving foundation for future decisions.

Knowledge of the attenuation relation used to define the decay of p.g.a. over distance has also developed substantially. The MB attenuation model used in Makropoulos and Burton [27] in fact adapted relations derived from areas other than Greece for use in Greece, demonstrating compatibility with the then existing Greek strong motion data. New attenuation relations have been derived for Greece and adjacent regions [2,3,43–45] relying on earthquake strong motion data recorded in Europe, in compatibly similar seismotectonic regions, and explicitly in Greece itself. It is vital to exploit these new developments in locally applicable attenuation laws alongside an extended and improved earthquake catalogue.

We have a third reason in that embarking on an earthquake early warning demonstration shield for the Revithoussa liquid natural gas hydrocarbon storage site in Greece, adjacent to Athens, it is necessary to perform a strategic seismic hazard assessment. The role of seismic hazard analyses in the design of an earthquake early warning system needs careful consideration. It should be apparent that this role is not simply one of conventional seismic hazard estimation alone. Seismic hazard assessment combined with earthquake scenario selection can go much beyond this, it can characterize seismogenic zones and then rank their implicit impact potential on the shielded site or facilities, and directly aid the identification of the optimal sites on which to deploy the instrumental sensors of the shield—it can also characterize the seismicity for which the Shield should be on the alert. The use of p.g.a. seismic hazard results is only one strand in such a strategic assessment, but these results will be determined here.

The next consideration is that the extensive results from the Global Seismic Hazard Assessment Programme (GSHAP) include the first global map of seismic hazard [19]. This global map provides the p.g.a. that has a 10% chance of exceedance in 50-year (i.e. often taken to correspond to a '475-year return period'). The map has been put together from a set of regional analyses and maps

of seismic hazard and Greece is considered as part of two contributory papers, [17,41]. Slejko et al. addresses the region of Adria. This is defined to extend from the Alps in the north ($\sim 48°$N) to the Ionian abyssal plain to the south ($\sim 36°$N), the Apennines in the west ($\sim 6°$W) and east across the Adriatic to as far as the Cephalonia escarpment ($\sim 24°$W)—the most hazardous zone is Cephalonia of Greece. No further eastward area of Greece is analyzed. The catalogue of Makropoulos and Burton [25] was preferred for post-1900 instrumental determinations in Greek territory. Several strong ground attenuation motion relations were considered but that of Ambraseys et al. [4] preferred because of the wide extent of the strong motion data set employed to calibrate it for Europe, and secondly because it spans a wide magnitude range. Epicentral distance was usually substituted for the distance from the fault (specified in the actual attenuation law) except at the large magnitudes when actual fault distance could be computed. In the other GSHAP paper, Erdik et al. [17] perform their seismic hazard analysis for Turkey and neighboring regions. This actually encompasses Turkey, from the Aegean region in the west to the Caucasus in the east, embraces all of mainland Greece, extending west to $\sim 19°$E, and Crete, extending south to $\sim 34°$S. Three recently derived p.g.a. attenuation relationships are adopted by Erdik et al., with equal weight assigned to attenuation laws of Boore et al. [10], Campbell [14] and Sadigh et al. [38]. Campbell used strong motion data from worldwide active tectonic regions, Boore et al. analyze shallow earthquakes in western North America and Sadigh et al. also analyze strong motion data primarily from earthquakes in California: none of these sources lean towards analysis of European strong motion data. The regional seismicity analyzed by Erdik et al. of course includes the tectonic belt of the North Anatolian Fault (and the East Anatolian Fault) and there is a need for strong motion data from major strike-slip sources. The results of Spudich et al. [42], who determine attenuation laws explicitly for extensional regimes, is not included, although they include data from earthquakes that have occurred along extensional offsets in the Anatolian fault system. It appears, understandably, that neither Slejko et al. [41] nor Erdik et al. [17] had Greece as their main focus. The GSHAP seismic hazard analyses that span the territory of Greece are not entirely focused on problems specific to mainland Greece and the GSHAP map thus provides a suitable basis for development and comparison of results with future regionally specific analyses in this area.

The fifth reason is that the New Greek Seismic Code (NEAK) was passed by the Greek parliament in 1992, and came into force in 1996. NEAK adopted a seismic hazard zoning map of Greece, based on p.g.a. values and intensity, and this is illustrated in Fig. 1. Our new results will provide a comparison with NEAK.

Finally, there is the advent of the work of Papaioannou and Papazachos [34] who have investigated seismic hazard
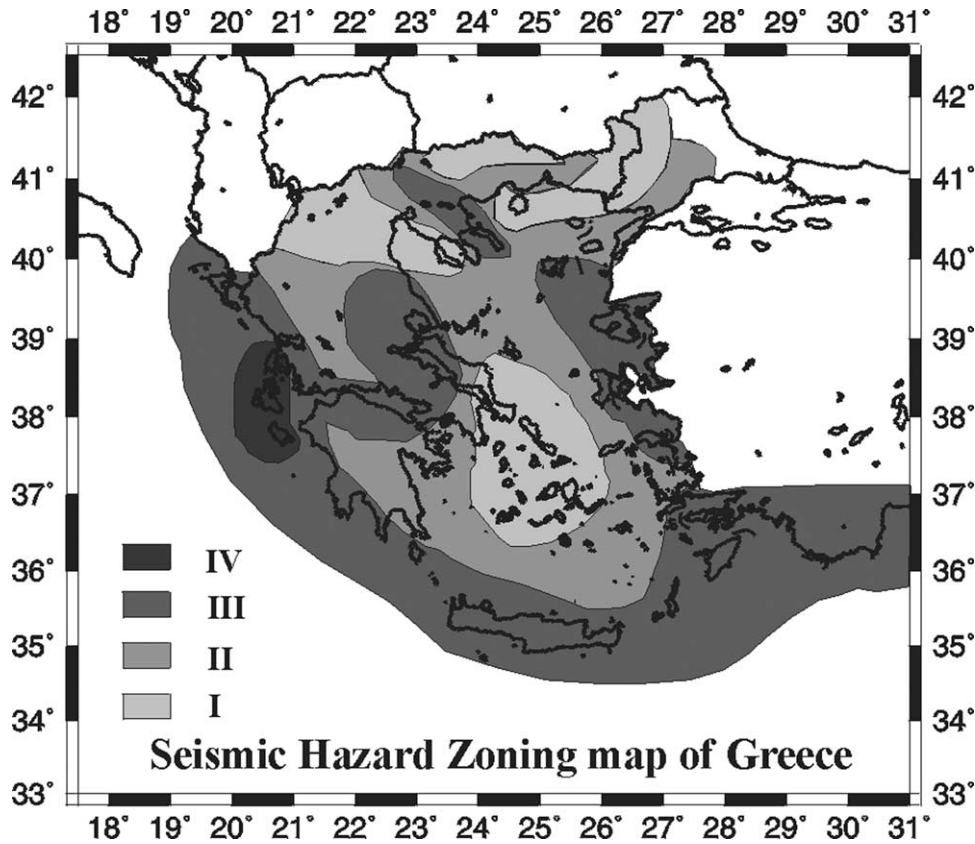
Fig. 1. Seismic hazard zoning map of Greece adapted from the New Greek Seismic Code (NEAK). NEAK addresses average horizontal p.g.a. values (%g) for a mean-return period of 475-year and adopts four zones: Zone I 12%g, Zone II 16%g, Zone III 24%g, Zone IV 36%g.

in Greece using both time-independent and time-dependent models. They produce results for 144 broad sites. Crucially, they relied on defining seismogenic sources or zones of which there are 67 (for shallow earthquakes) in total whereas we intend to provide results from a *zone-free* seismic hazard analysis in the present work.

The paper is ordered to set out a brief description of the basic extreme value method, as this is well known, and the data. Then it provides results using the MB attenuation model for comparison with the existing Makropoulos and Burton [27] results, followed by examination of new attenuation laws, their more obvious implications and attributes, and production of corresponding p.g.a. results. Many of the results are in the form of p.g.a. values mapped over Greece and most of the discussion of these maps takes place in combined manner towards the end of the paper. The p.g.a. hazard results are always produced for a 50-year period with 10% probability of exceedance as has become conventional. However, this is an entirely arbitrary benchmark that will not satisfy all needs and all users; so other levels of hazard statistic are presented in the city-specific tables and in the final selection of preferred p.g.a. hazard maps. Not all the maps produced and used during the course of this research can be included here.

2. Method and data

The extreme value statistics described by Gumbel [20] are used for this study. The first of Gumbel's asymptotic extreme value distributions (Gumbel I) is given by

$$G^{\mathrm{I}}(a) = \exp\{ -\exp[-\alpha(a - u)]\} \qquad (1)$$

where α and the characteristic modal extreme, u, are the two parameters of this distribution, and G is the probability that a is an annual extreme of p.g.a. at a point. Values of a are determined using an appropriate p.g.a. attenuation law and annual extremes of a, at each site or point of interest, are extracted from the whole suite of a values determined from each earthquake for the site of interest.

The p.g.a. expected to be the annual maximum with probability P is then given by

$$a_{\mathrm{p}} = u - [\ln(-\ln P)]/\alpha \qquad (2)$$

or the p.g.a. which has probability P of not being exceeded in T-year is

$$a_{\mathrm{P,T}} = u - [\ln(-\ln P)]/\alpha + (\ln T)/\alpha = a_p + (\ln T)/\alpha \qquad (3)$$

The Gumbel III distribution is not used with annual maximum accelerations because this usually results in

poor convergence, with values of the curvature parameter, λ, close to zero [27].

The earthquake catalogue adopted is an updated MB earthquake catalogue for Greece spanning 1900–1999 [13]. The primary MB catalogue spans 1901–1978 and its strength is 605 earthquakes uniformly relocated for the period 1917–1963 and magnitudes uniformly redetermined from 1908 onwards [25,28]. Results from the International Seismological Center (ISC) were then adopted from 1964 onwards. The basic sources used for the present updated catalogue are the ISC, National Earthquake Information Center (NEIC) and the CMT Harvard catalogues. The National Observatory of Athens (NOA) catalogue is used for the most recent small events. Also consulted are Engdahl et al. [16], Pérez [37], and some recent Greek seismological results [7,31,36] to improve on qualities such as accuracy, completeness and homogeneity. A fundamental need was to be able to convert different magnitude scales used by different sources in the more recent years and, with such conversions in place, a catalogue for the period 1900–1999 AD is produced. This catalogue contains magnitudes for all earthquakes, on both moment magnitude and surface wave magnitude scales, whether reported, observed or converted values; also included are any reported observed magnitudes on any of the scales M_W, M_S, m_b and M_L. This catalogue contains a total of 7079 earthquakes during 1900–1999 AD, within the area 33.00–43.00°N, 18.00–30.99°E, focal depths 1.0–350.0 km and magnitude range $2.1 \leq M_W \leq 7.7$. This working catalogue is then censored to accept only events with magnitudes $M_W \geq 4.0$. Truncation at $4.0M_W$, rather than at $4.0M_S$, is preferred because scale conversion equations suggests $4.0M_W \cong 2.4M_S$ while $4.0M_S \cong 4.9M_W$ and it was deemed preferable not to eliminate earthquakes in the magnitude range 4.0–4.9, no matter what scale or conversion generated them, i.e. $4.0M_W < 4.0M_S$. This censored catalogue contains a total of 5198 earthquakes during 1900–1999 AD, within the area 33.00–43.00°N, 18.00–30.99°E, focal depths 1.0–215.0 km and magnitude range $4.0 \leq M_W \leq 7.7$. A description of the details of production of this new catalogue, and the catalogue itself, can be made available on CDROM. The surface wave magnitude, M_S, is used to characterize earthquakes in this analysis because this scale dominates most analyses of earthquake strong motion data producing p.g.a. attenuation laws. This updated catalogue is used here to compute p.g.a. at a point of interest associated with each event.

3. Peak ground acceleration hazard evaluation using the MB attenuation model

3.1. MB attenuation model

The MB attenuation model for Greece was derived from a few well-known formulae which had resulted from worldwide studies; this was because the limited number of strong motion records then available in Greece did not permit a regional study of attenuation of ground vibration. This model or formula is given by

$$a = 2164 \ e^{0.7M_S}(r + 20)^{-1.80} \tag{4}$$

where a cm s^{-2} is p.g.a., M_S is the earthquake magnitude and r is hypocentral distance in km. This attenuation law is an average of eight independent attenuation laws used to describe the attenuation of p.g.a. by various authors in the mid-1970s [1,9,15,24,33,39,49]. This average law was demonstrably compatible with the few observations of strong ground motion then available in Greece. In most of what follows the horizontal p.g.a. a_h is used.

The earthquake records (1900–1999, $M_S \geq 5.5$) and (1964–1999, $M_S \geq 4.0$) are taken as best samples of complete data for Greece [25,28,34,36] and these are adopted here as the magnitude thresholds appropriate for analysis.

3.2. Acceleration seismic hazard at six cities from the MB model

The results for p.g.a.s which have 70 or 90% probability of not being exceeded in T-years, where T is 25, 50, 100 and 200-year, for six important cities and Revithoussa in Greece are listed in Table 1. The return periods T' corresponding to T-year events with probabilities P of non-exceedance are listed in Table 2, to help interpretation of these hazard levels, noting that $T' = 1/(1 - P^{1/T})$. The magnitude thresholds used during analysis are $M_S \geq 4.0$ and $M_S \geq 5.5$ for the earthquake catalogue periods 1900–1999 and 1964–1999, respectively. These results compare consistently well with those of Makropoulos and Burton [27]. Generally, the p.g.a. values for data 1964–1999 are slightly smaller than the corresponding values for data 1900–1999.

Acceleration values emboldened in Table 1 correspond to results from analysis of the earthquake catalogue for 1900–1999 with a $5.5M_S$ threshold, the best data span available, and to forecasts of the 50-year event with 90% non-exceedance probability (one chance in ten of exceedance). This corresponds to the event with an average return period of 475-year, which has become an arbitrarily accepted and typical norm for hazard comparisons. Among these six cities, Athens, Corinth and Patras are located in the central belt dominated by the Gulf of Corinth Seismic Zone. The representative acceleration, $a_{P,T} \equiv a_{0.9,50}$ for Patras (data 1900–1999, threshold $M_S \geq 5.5$, $T = 50$-year with $P = 90\%$) is about 130 cm s^{-2}. This is quite a high value. The corresponding $a_{0.9,50}$ p.g.a. value for Athens is 126 cm s^{-2}, with a lower value of 94 cm s^{-2} resulting if only the more recent data are considered (1964–1999, $M_S \geq 4.0$). The corresponding representative $a_{0.9,50}$ p.g.a. value for

Table 1
Peak ground accelerations, cm s^{-2}, which have 70 and 90% probability of non-exceedance in T-year, based on the MB attenuation model

City	$T = 25$-year	$T = 50$-year	$T = 100$-year	$T = 200$-year	Comment
Athens, 37.97N, 23.72E	79.93	92.39*	104.85	117.32	MB
	67.09	76.77	86.46	96.15	$M_S \geq 4.0$, 1964–1999, 70%
	84.39	99.33*	114.27	129.21	$M_S \geq 5.5$, 1900–1999, 70%
	84.13	93.82	103.50	113.19	$M_S \geq 4.0$, 1964–1999, 90%
	110.68	**125.62**	140.56	155.49	$M_S \geq 5.5$, 1900–1999, 90%
Corinth, 37.92N, 22.93E	117.87	136.27*	154.67	173.07	MB
	129.69	148.48	167.26	186.05	$M_S \geq 4.0$, 1964–1999, 70%
	131.14	154.16*	177.18	200.20	$M_S \geq 5.5$, 1900–1999, 70%
	162.74	181.53	200.32	219.11	$M_S \geq 4.0$, 1964–1999, 90%
	171.64	**194.66**	217.67	240.69	$M_S \geq 5.5$, 1900–1999, 90%
Heraklion, 35.35N, 25.18E	55.93	63.73*	71.52	79.32	MB
	41.76	46.95	52.14	57.33	$M_S \geq 4.0$, 1964–1999, 70%
	48.37	56.23*	64.09	71.95	$M_S \geq 5.5$, 1900–1999, 70%
	50.89	56.08	61.28	66.47	$M_S \geq 4.0$, 1964–1999, 90%
	62.20	**70.06**	77.92	85.78	$M_S \geq 5.5$, 1900–1999, 90%
Patras, 38.23N, 21.75E	102.40	117.16*	131.92	146.68	MB
	117.74	133.95	150.15	166.35	$M_S \geq 4.0$, 1964–1999, 70%
	91.18	105.38*	119.57	133.77	$M_S \geq 5.5$, 1900–1999, 70%
	146.25	162.45	178.66	194.86	$M_S \geq 4.0$, 1964–1999, 90%
	116.16	**130.35**	144.55	158.75	$M_S \geq 5.5$, 1900–1999, 90%
Rodhos, 36.43N, 28.27E	63.88	73.15*	82.41	91.68	MB
	38.34	43.23	48.12	53.01	$M_S \geq 4.0$, 1964–1999, 70%
	60.17	70.20*	80.23	90.25	$M_S \geq 5.5$, 1900–1999, 70%
	46.94	51.83	56.72	61.61	$M_S \geq 4.0$, 1964–1999, 90%
	81.25	**92.75**	104.25	115.75	$M_S \geq 5.5$, 1900–1999, 90%
Thessaloniki, 40.64N, 22.93E	122.47	143.16*	163.85	184.54	MB
	81.07	94.72	108.38	122.04	$M_S \geq 4.0$, 1964–1999, 70%
	109.35	131.30*	153.25	175.20	$M_S \geq 5.5$, 1900–1999, 70%
	105.09	118.75	132.41	146.07	$M_S \geq 4.0$, 1964–1999, 90%
	147.97	**169.92**	191.87	213.82	$M_S \geq 5.5$, 1900–1999, 90%
Revithoussa, 37.96N, 23.40E	116.23	129.14	142.05	154.97	$M_S \geq 4.0$, 1964–1999, 90%
	163.31	**185.80**	208.29	230.78	$M_S \geq 5.5$, 1900–1999, 90%

Note: MB refers to Makropoulos and Burton model in which probabilities for T-year are computed at the 70% level.

Corinth is 195 cm s^{-2}, representing a high acceleration hazard from relatively near-field earthquakes of the Corinth Gulf. Although Athens does perceive earthquakes of the Corinth Gulf, it is relatively distant compared to Corinth. The $a_{0.9,50}$ p.g.a. value at Revithoussa is 186 cm s^{-2}, reflecting its position west of Athens and therefore closer to the Corinth Gulf seismicity.

Heraklion (Crete) and Rodhos are located in the south-eastern part of the Hellenic Seismic Arc. The representative $a_{0.9,50}$ p.g.a. value for Heraklion is 70 cm s^{-2} and for Rodhos is 93 cm s^{-2}, apparently low values, given the substantial seismicity of the arc, but such values arise because they are associated with earthquake focuses at intermediate depth, a factor which is allowed for through the attenuation model.

The overall change to results of site-specific seismic hazard analyses caused by an addition of 21 years of high quality earthquake catalogue data may be summarized through inspection of the values marked '∗' in Table 1. These values, city by city, compare 50-year p.g.a. values with 70% of non-exceedance (140-year average return period) determined by Makropoulos and Burton [27] and those in this paper using $M_S \geq 5.5$ during 1900–1999. The changes in this p.g.a. statistic are: Athens +7.5%, Corinth +13.1%, Heraklion −11.7%, Patras −10.1%, Rodhos −4.0%, Thessaloniki −8.3%. These changes are typically of order 10%. Only two of these major cities show an increase with an extra 21 years of data. These are Athens and Corinth which are associated with the earthquakes of Athens 1999 and Corinth 1981, respectively, during 1979–1999.

Maps of spatially distributed p.g.a. calculated using the MB model of attenuation will be considered later, along

Table 2
Average return periods T'-year corresponding to T-year events with 70 and 90% probabilities of non-exceedance

	$T = 25$-year	$T = 50$-year	$T = 100$-year	$T = 200$-year
T' at 70%	70	140	280	560
T' at 90%	238	475	950	1900

with maps resulting from other attenuation models—which will now be developed.

4. Horizontal peak ground acceleration described by 'Theodulidis–Papazachos' and 'Ambraseys' models of attenuation: 'TP' and 'AM' models

The attenuation law or model of horizontal peak acceleration derived by Makropoulos and Burton was introduced above as Eq. (4), where it was pointed out that this MB model incorporates relations derived for areas other than Greece. The development of earthquake strong motion recording has increased in Greece in recent years. For example, Kalogeras and Stavrakakis [23], ITSAK [22] and more recent work all report entirely on strong motion recordings of Greek earthquakes. The cited report of Kalogeras and Stavrakakis details strong motion recordings of the NOA for the period 1990–1994 and this is ongoing. These new databases lay a foundation to develop and test attenuation relationships appropriate to analysis of Greek seismic hazard and new attenuation relations have emerged that are derived from earthquake strong motion data in Europe and explicitly in Greece.

The results of Theodulidis and Papazachos [44] were obtained directly using 105 horizontal records from 36 shallow earthquakes in Greece, with magnitudes 4.5–7.0, (plus a further 16 horizontal components from four shallow subduction earthquakes in Japan and Alaska, 7.2–7.5 M) and provide:

$$\ln(a_h) = 3.88 + 1.12M_S - 1.65 \ln(R+15) + 0.41S + 0.71P \tag{5}$$

where a_h is the peak horizontal acceleration in cm s^{-2}, R is epicentral distance in km, S is equal to zero at 'alluvium' sites and equal to one at a 'rock' site, and P is zero for mean or 50-percentile values and one for 84-percentile values. Eq. (5) is one of the set of new models of attenuation that was explored and applied to the production of acceleration hazard values and maps for Greece in this study. Concern over p.g.a. values obtained at alluvial and rock sites resulted in further explanation from Theodulidis (written communication) than is available in Theodulidis and Papazachos [44]. Theodulidis points out that the majority of earthquake strong motion data available to them for regression in 1992 and characterized as a rock site was subsequently found by geotechnical investigation to be perturbed by a thin layer ($\sim$ 10 m) of weathered material that amplified strong motion around 5–7 Hz, in the frequency range where p.g.a. values were observed. This thin layer did not affect peak ground velocity and displacement as they appear at lower frequencies, but the p.g.a. attenuation model for rock sites may be biased by this site. Theodulidis recommends (written communication) use of an average ($P = 0$) attenuation model for p.g.a. as representative for stiff soil

conditions obtained by setting $S = 0.5$. The recommended stiff soil p.g.a. attenuation model of Theodulidis is thus

$$\ln(a_h) = 4.09 + 1.12M_S - 1.65 \ln(R+15) \tag{5a}$$

Ambraseys ([3], also see the material developed in: [2,4–6]) supplies the equation for horizontal accelerations

$$\log(a_h) = -1.05 + 0.245M_S - 0.001r - 0.786 \log(r)$$
$$+ E \log(V_S30) + 0.23P \tag{6}$$

Ambraseys [3] also cites P as 0 for 50-percentiles and 1 for 84-percentiles, $r^2 = d^2 + h_o^2$ in km, $h_o = 2.7$, and a_h is expressed in g. Source distance, d km, is defined here to be the closest distance to the surface projection of the fault rupture (noting that the Authors used epicentral distance for small events because the source dimensions of small magnitude crustal earthquakes imply negligible difference between epicentral and source distance). The term $E \times \log(V_S30)$ with $E = -0.15$ simulates the role of a magnification coefficient for different sites defined by their average shear wave velocity at a reference depth of 30 m, i.e. the upper 30 m. These station shear wave velocities ranged from 149 m s^{-1} for Edesa in Greece to 1110 m s^{-1} at Bagnioli in Italy. Of the 268 records used, Ambraseys points out that only 14 are at source distances exceeding 40 km, thus it is difficult to extrapolate this equation to greater distances. Perhaps Eq. (6), although somewhat experimental, is appropriate for assessment of p.g.a. hazard near to the earthquake source, one application of this would be for some earthquake early warning stations in a Shield which are intended to be deployed near-source. To summarize Ambraseys and co-workers' findings for zero-period horizontal acceleration, there are the four following equations for Europe most relevant to this p.g.a. hazard study, and all derived with E of Eq. (6) set to zero

$$\log(a_h) = -1.429 + 0.245M_S - 0.00103r - 0.786$$
$$\log(r) + 0.241P \tag{6a}$$
$$\log(a_h) = -1.242 + 0.238M_S - 0.00005r - 0.907$$
$$\log(r) + 0.240P \tag{6b}$$
$$\log(a_h) = -1.060 + 0.245M_S - 0.00045r - 1.016$$
$$\log(r) + 0.254P \tag{6c}$$
$$\log(a_h) = -0.895 + 0.215M_S - 0.00011r - 1.070$$
$$\log(r) + 0.247P \tag{6d}$$

Eqs. 6(a) and (6b) are calculated without depth control, in M_S magnitude ranges 4.0–7.3 and 5.0–7.3, respectively. h_o is 2.66 and 4.04 in $r^2 = d^2 + h_o^2$ in Eqs. 6(a) and (6b), respectively. Eqs. (6c) and (6d) are calculated with depth control using $r^2 = d^2 + h^2$ (r is slant distance to the source using focal depth h; there is no h_o), and in M_S magnitude ranges 4.0–7.3 and 5.0–7.3, respectively. Standard

deviations on log(a_h) are 0.241, 0.240, 0.254, 0.247 in Eqs. (6a)–(6d). The value of a_h predicted is the maximum of the two horizontal components. An estimate of the mean of the maximum of the two horizontal components is obtained by multiplying by 0.8. Of these Eqs. (6b) and (6d) are more appropriate to analyze horizontal p.g.a. seismic hazard by our extreme value approach, since magnitudes under $5M_S$ are unlikely to cause damage and be of engineering concern.

4.1. Comparison of the suite of attenuation relationships

Fig. 2(a) shows p.g.a. decaying with distance for a representative earthquake of magnitude $6.5M_S$ at focal depth $h = 10$ km. Nine conditions of the attenuation laws of Makropoulos and Burton (MB), Ambraseys et al. (AM) and Theodulidis and Papazachos (TP) are illustrated. These nine conditions are

1. Makropoulos and Burton: Eq. (4), mean value or 50-percentile MB
2. Theodulidis and Papazachos: Eq. (5), rock site, 50-percentile TP
3. Theodulidis and Papazachos: Eq. (5), rock site, 84-percentile TP84
4. Theodulidis (written comm.): Eq. (5a), stiff soil site, 50-percentile NTP
5. Theodulidis (written comm.): Eq. (5a), stiff soil site, 84-percentile NTP84
6. Ambraseys et al.: Eq. (6b) [no depth control],rock site, 50-percentile AM1
7. Ambraseys et al.: Eq. (6b) [no depth control], rock site, 84-percentile AM1_84
8. Ambraseys et al.: Eq. (6d) [depth control], rock site, 50-percentile AM2
9. Ambraseys et al.: Eq. (6d) [depth control], rock site, 84-percentile AM2_84

Plotting 84-percentiles for four curves in Fig. 2(a) reveals the level of dispersion in the data encompassed by the different data sets. The dispersion in the Ambraseys et al. data set is less, but similar to that of the Theodulidis and Papazachos data set. Seeking extra confidence in calculated p.g.a. values using the dispersed laws at the 84% value would usually approximately double p.g.a. values. Using such high p.g.a. values as
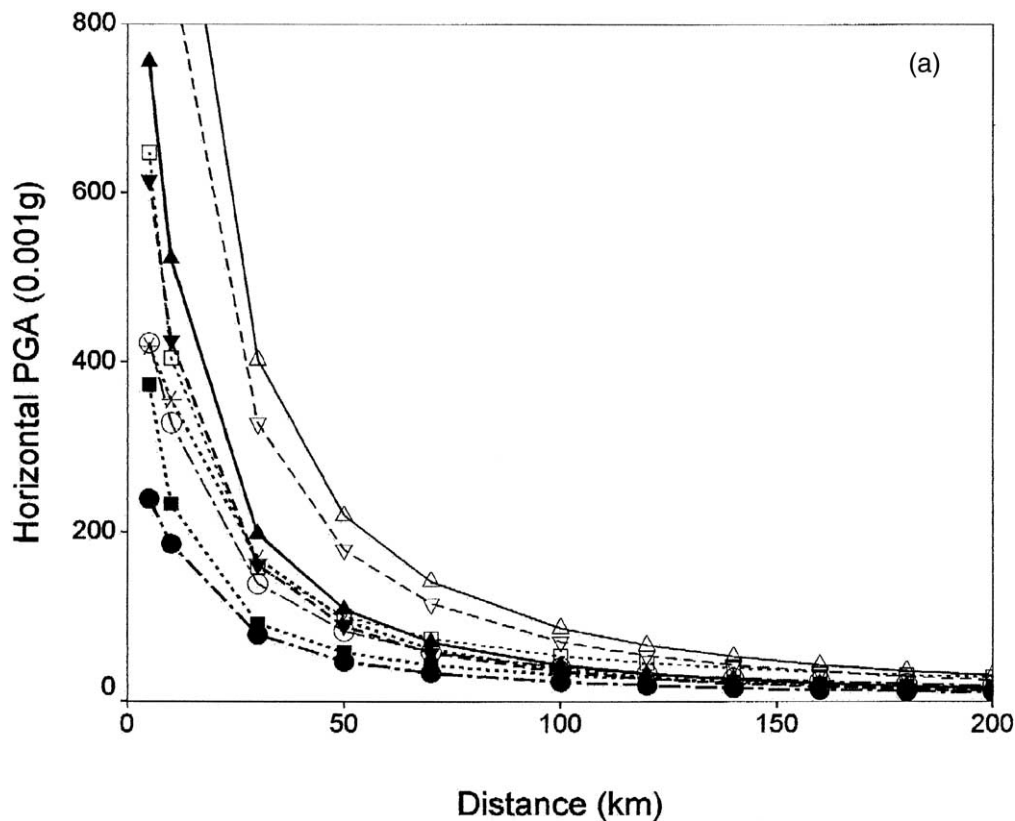

Fig. 2. Attenuation relations investigated for Greece. Individual curves are: *: Makropoulos and Burton: Eq. (4), mean value [MB]; (▲): Theodulidis and Papazachos: Eq. (5), rock site, 50-percentile [TP]; (△): Theodulidis and Papazachos: Eq. (5), rock site, 84-percentile [TP84]; (▼): Theodulidis (written comm.): Eq. (5a), stiff soil site, 50-percentile [NTP]; (▽): Theodulidis (written comm.): Eq. (5a), stiff soil site, 84-percentile [NTP84]; (■): Ambraseys et al.: Eq. (6b) [no depth control], rock site, 50-percentile [AM1]; (□): Ambraseys et al.: Eq. (6b) [no depth control], rock site, 84-percentile [AM1_84]; (●): Ambraseys et al.: Eq. (6d) [depth control], rock site, 50-percentile [AM2]; (○): Ambraseys et al.: Eq. (6d) [depth control], rock site, 84-percentile [AM2_84]: (a) all nine attenuation laws for an earthquake $6.5M_S$ at focal depth $h = 10$ km; (b) as (a) but excluding the four curves at 84-percentile values; (c) as (b) but at focal depth $h = 0$ km. See text for details.
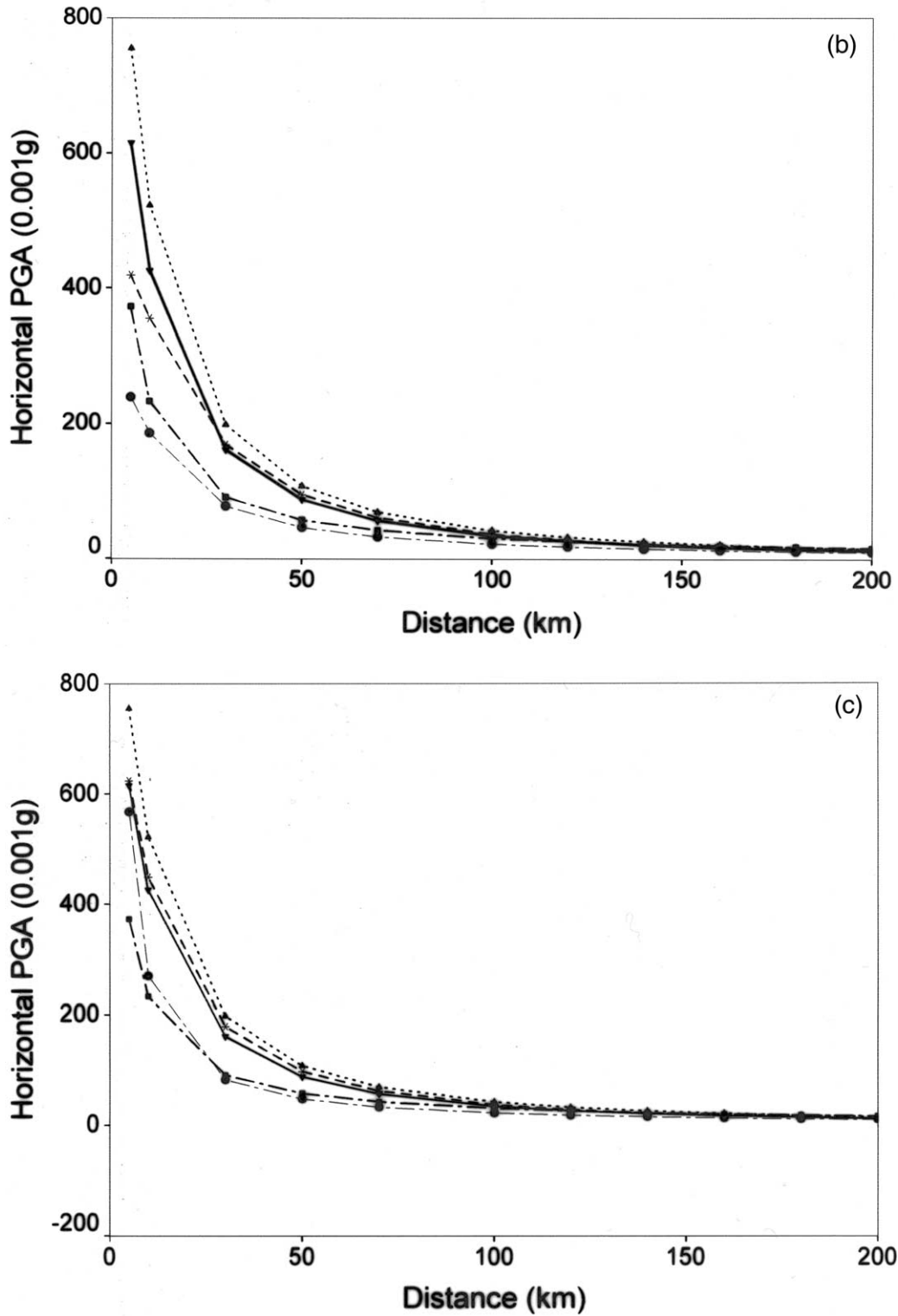
Fig. 2 (*continued*)

representative would also preclude comparison of ensuing results with values in the NEAK map. The 84-percentile curves are considered unsuitable for this stage of seismic hazard analysis and the five mean or 50-percentile curves are adopted. These are separately shown in Fig. 2(b) for

the $h = 10$ km case and also in Fig. 2(c) for a notional surface focus $h = 0$ case.

It is clear from Fig. 2(b) and (c) that the attenuation relation (TP) of Theodulidis and Papazachos obtained directly from mostly Greek data is quite similar to

the curve MB, a relation that was derived from other areas and adapted to Greece. The attenuation relation AM1 derived from European data without depth control is close to AM2, derived from European data with depth control. The new Theodulidis and Papazachos attenuation relation (NTP, Theodulidis written communication) lies between TP and MB at distances less then 35 km in Fig. 2(b) for $h = 10$ km and is extremely close to MB for $h = 0$ in Fig. 2(c). The p.g.a. values represented by the three curves TP, MB and NTP are at face value quite similar to, and span, the values corresponding to Greek experience in the NEAK map, whereas those represented by the curves AM1 and AM2 are substantially less then the previous three at distances less than 50 km and are likely to produce values much smaller than, and incompatible with those in the NEAK map. Although all of these attenuation relations will be investigated further, the Eqs. (4), (5) and (5a) are adopted later as most appropriate to analyze and produce maps of spatial p.g.a. seismic hazard by our extreme value approach.

4.2. Acceleration hazard at six cities from the 'TP' and 'AM' models

Similarly to Table 1, results in Table 3 provide p.g.a.s which have 70 or 90% probability of not being exceeded in T-years, where T is 25, 50, 100 and 200-year, for six important cities and Revithoussa in Greece, using these newly developed attenuation relations. The magnitude thresholds used are again $M_S \geq 4.0$ and $M_S \geq 5.5$ for the earthquake catalogue periods 1900–1999 and 1964–1999 respectively. These results compare consistently well with those of Makropoulos and Burton [27]. As with the MB relationship (Table 1), in general the p.g.a. values for data 1964–1999 are slightly smaller than the corresponding values for data spanning 1900–1999. The exception is again Patras; the reason being increased strong shaking and seismicity since 1964, including the moderate urban earthquake of 1993 July 14 ($5.4M_S$, Tselentis et al. [51]). Results from the AM1 and AM2 models are usually substantially less than from the TP and NTP models in Table 3 and from MB in Table 1 (e.g. consider the arbitrary norm of 50-year, 90% probability non-exceedance level column).

5. Spatially distributed peak ground acceleration expectation in Greece

The area of Greece is notional here and taken to span 33.00–43.00°N, 18.00–31.00°E. This area is divided into a mesh of grid points at 0.5° intervals of latitude and longitude, all earthquakes above some reasonable magnitude threshold are then selected within 2° of each grid point for calculation of the corresponding p.g.a.s. These acceleration values are determined at the grid point based on the selected attenuation relationship or model, and the Gumbel distribution is then fitted to ranked annual extreme p.g.a. values.

5.1. Seismic hazard evaluations and maps derived from the 'MB' model

Results obtained from the MB attenuation relationship of Eq. (4) are shown in Figs. 3 and 4. The arbitrary contemporary norm for p.g.a. seismic hazard is to adopt the value with a 475-year average return period and this is displayed in Fig. 3(a).

The technical content of Figs. 3 and 4 is as follows. Maximum p.g.a. values with a 90% probability of not being exceeded (p.n.b.e.) in the next 50, 100 and 200-year for earthquakes during 1900–1999 with magnitude $M_S \geq 5.5$ are shown in Fig. 3(a)–(c); the 50-year p.g.a. value with 90% p.n.b.e. calculated using earthquakes during 1964–1999 with magnitude $M_S \geq 4.0$ is Fig. 3(d). In general Fig. 3(a)–(c) show a similar pattern with the corresponding p.g.a. value increasing proportionally to its previous values as the time increases through 50-, 100- to 200-year, because the expected value of maximum acceleration increases as a linear function of the logarithm of time [27]. Fig. 4(a) and (b) are the results for maximum p.g.a. values with 70% p.n.b.e. during the next 50-year, 70% being the statistic adopted by Makropoulos and Burton [27]. These two figures contrast results for different data lengths and magnitude thresholds, Fig. 4(a) representing earthquakes for the full period of 1900–1999 but with the higher magnitude threshold of $M_S \geq 5.5$, whereas Fig. 4(b) shows earthquakes observed and parameters determined during the 'modern' era 1964–1999 with a lower magnitude threshold of $M_S \geq 4.0$.

The following results are derived from the analysis of the maximum expected p.g.a. with 90% probability of not being exceeded in 50-year and are drawn simply from inspection of Figs. 3(a) and 4(a). Several different zones can be identified in these maps and these will need to be compared with the NEAK seismic hazard zones expressed in Fig. 1. However, some zones with high p.g.a. values will be considered first.

The first zone of note with high p.g.a. values in Fig. 3(a) is along the western Hellenic Arc. Values exceeding 200 cm s^{-2} dominate Levkas–Cephalonia–Zakinthos islands and Albania. Of particular note is Cephalonia–Zakinthos islands, which display the highest values in the region exceeding 300 cm s^{-2}. It should be noted that the values further southeast along the Hellenic Arc in Crete are smaller than might be expected, in view of the expected large magnitudes of earthquakes occurring there, because focal depths are also quite large. The NEAK map in Fig. 1 places Levkas–Cephalonia–Zakinthos islands in their zone with the highest values, Hazard Zone IV (p.g.a. value 36%g, about 350 cm s^{-2}, [34]). These values are very similar and mutually corroborative. The NEAK map places the remainder of the Hellenic Arc in NEAK Hazard Zone III (p.g.a. value 24%g, about 235 cm s^{-2}) but Fig. 3(a) usually shows lesser values than this, particularly in the central and further eastern areas of the Hellenic Arc.

Table 3
p.g.a.s, cm s^{-2}, which have 90% probability of non-exceedance in T-year, based on the TP and AM attenuation models

City	$T = 25$-year	$T = 50$-year	$T = 100$-year	$T = 200$-year	Comment
Athens, 37.97N, 23.72E	189.33	212.50	235.68	258.85	TP_1
	202.49	231.54	260.59	289.64	TP_2
	154.24	173.11	192.00	210.87	NTP_1
	164.96	188.62	212.29	235.95	NTP_2
	116.59	129.89	143.19	156.49	AM1_1
	117.29	132.94	148.58	164.23	AM1_2
	46.47	51.21	55.95	60.68	AM2_1
	106.09	120.36	134.63	148.90	AM2_2
Corinth, 37.92N, 22.93E	222.73	248.76	274.80	300.83	TP_1
	309.95	353.28	396.60	439.93	TP_2
	181.45	202.65	223.87	245.07	NTP_1
	252.50	287.80	323.09	358.39	NTP_2
	132.37	146.35	160.34	174.33	AM1_1
	145.05	163.76	182.47	201.17	AM1_2
	82.92	91.71	100.50	109.30	AM2_1
	86.72	97.73	108.75	119.77	AM2_2
Heraklion, 35.35N, 25.18E	167.59	187.33	207.07	226.81	TP_1
	242.09	279.48	316.87	354.26	TP_2
	136.53	152.61	168.69	184.77	NTP_1
	197.22	227.68	258.14	288.60	NTP_2
	90.12	99.82	109.51	119.21	AM1_1
	86.18	97.31	108.43	119.56	AM1_2
	31.68	34.45	37.22	39.98	AM2_1
	35.49	39.48	43.46	47.45	AM2_2
Patras, 38.23N, 21.75E	215.57	240.81	266.05	291.29	TP_1
	197.83	223.89	249.96	276.03	TP_2
	175.61	196.18	216.74	237.30	NTP_1
	161.16	182.39	203.63	224.87	NTP_2
	150.49	167.03	183.57	200.10	AM1_1
	120.16	134.90	149.65	164.40	AM1_2
	89.87	99.39	108.90	118.42	AM2_1
	63.28	70.53	77.78	85.03	AM2_2
Rodhos, 36.43N, 28.27E	86.47	96.39	106.31	116.23	TP_1
	235.37	272.99	310.62	348.24	TP_2
	70.44	78.52	86.61	94.69	NTP_1
	191.74	222.39	253.05	283.69	NTP_2
	87.58	96.87	106.16	115.45	AM1_1
	103.87	118.69	133.51	148.34	AM1_2
	31.58	34.34	37.10	39.86	AM2_1
	43.53	49.10	54.67	60.23	AM2_2
Thessaloniki, 40.64N, 22.93E	89.76	100.80	111.84	122.88	TP_1
	183.37	210.91	238.45	265.99	TP_2
	73.12	82.12	91.11	100.10	NTP_1
	149.38	171.82	194.25	216.69	NTP_2
	71.50	79.45	87.40	95.34	AM1_1
	89.06	100.97	112.88	124.79	AM1_2
	64.81	72.26	79.71	87.16	AM2_1
	72.99	83.14	93.29	103.44	AM2_2
Revithoussa, 37.96N, 23.40E	161.64	180.56	199.48	218.40	TP_1
	218.43	248.65	278.87	309.08	TP_2
	131.68	147.09	162.51	177.92	NTP_1
Revithoussa, 37.96N, 23.40E	177.94	202.56	227.18	251.79	NTP_2
	101.21	111.93	122.65	133.38	AM1_1
	116.27	131.00	145.72	160.45	AM1_2
	64.70	71.47	78.25	85.02	AM2_1
	82.15	92.83	103.51	103.51	AM2_2

Note: TP refers to Theodulidis and Papazachos models, 50-percentile values at "rock" sites with TP_1: Data (Ms≥4.0, 1964–1999) and TP_2: Data (Ms≥5.5, 1900–1999). NTP_1 and NTP_2 refer with similar data convention to the TP models modified to "stiff soil" sites. AM1 and AM2 refer to Ambraseys et al. models without and with depth control respectively, 50-percentile values at "rock" sites, with AM1_1 and AM2_1: Data (Ms≥4.0, 1964–1999), AM1_2: and AM2_2: Data (Ms≥5.5, 1900–1999).
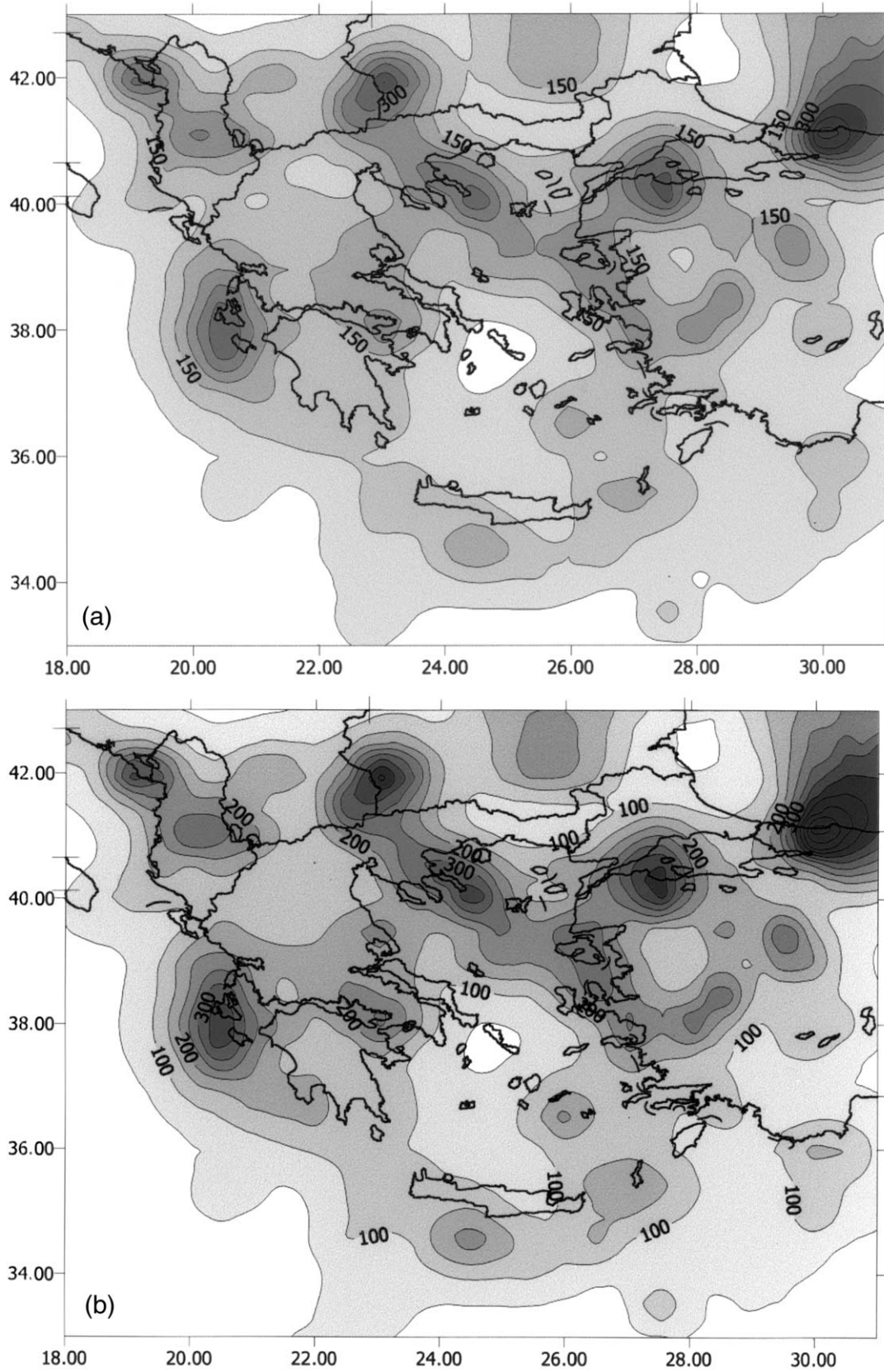
Fig. 3. Seismic hazard maps for Greece using the MB attenuation relationship. Contours are expected maximum p.g.a.s (p.g.a. cm s^{-2}) with 90% probability of not being exceeded (p.n.b.e.) during time periods: (a) 50-year; (b) 100-year and (c) 200-year, using data 1900–1999 with $M_S \geq 5.5$; (d) is 90% p.n.b.e. during 50-year using data 1964–1999 with $M_S \geq 4.0$.
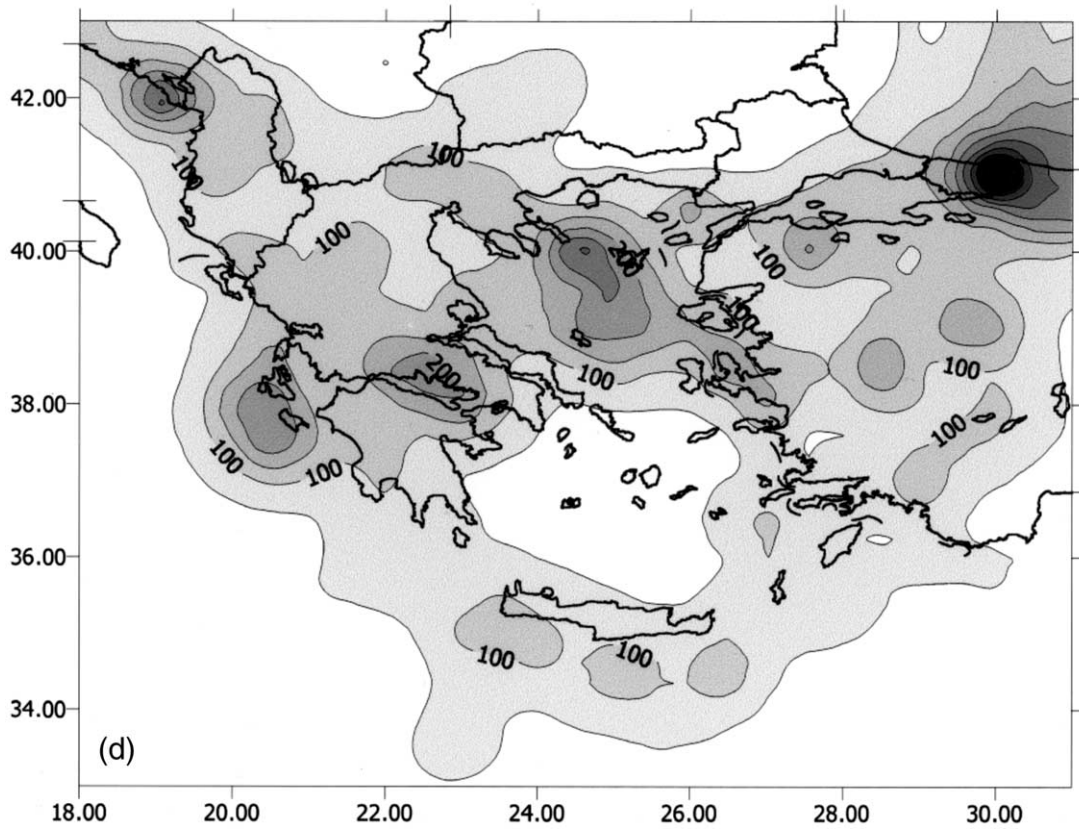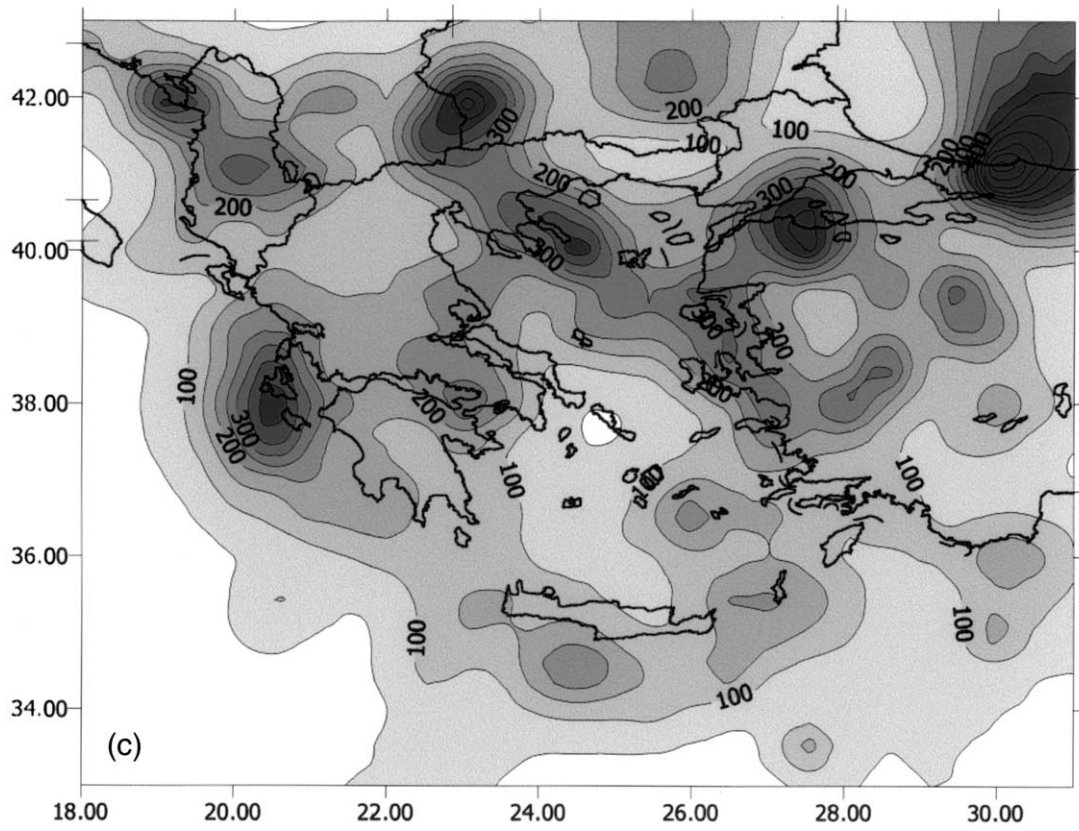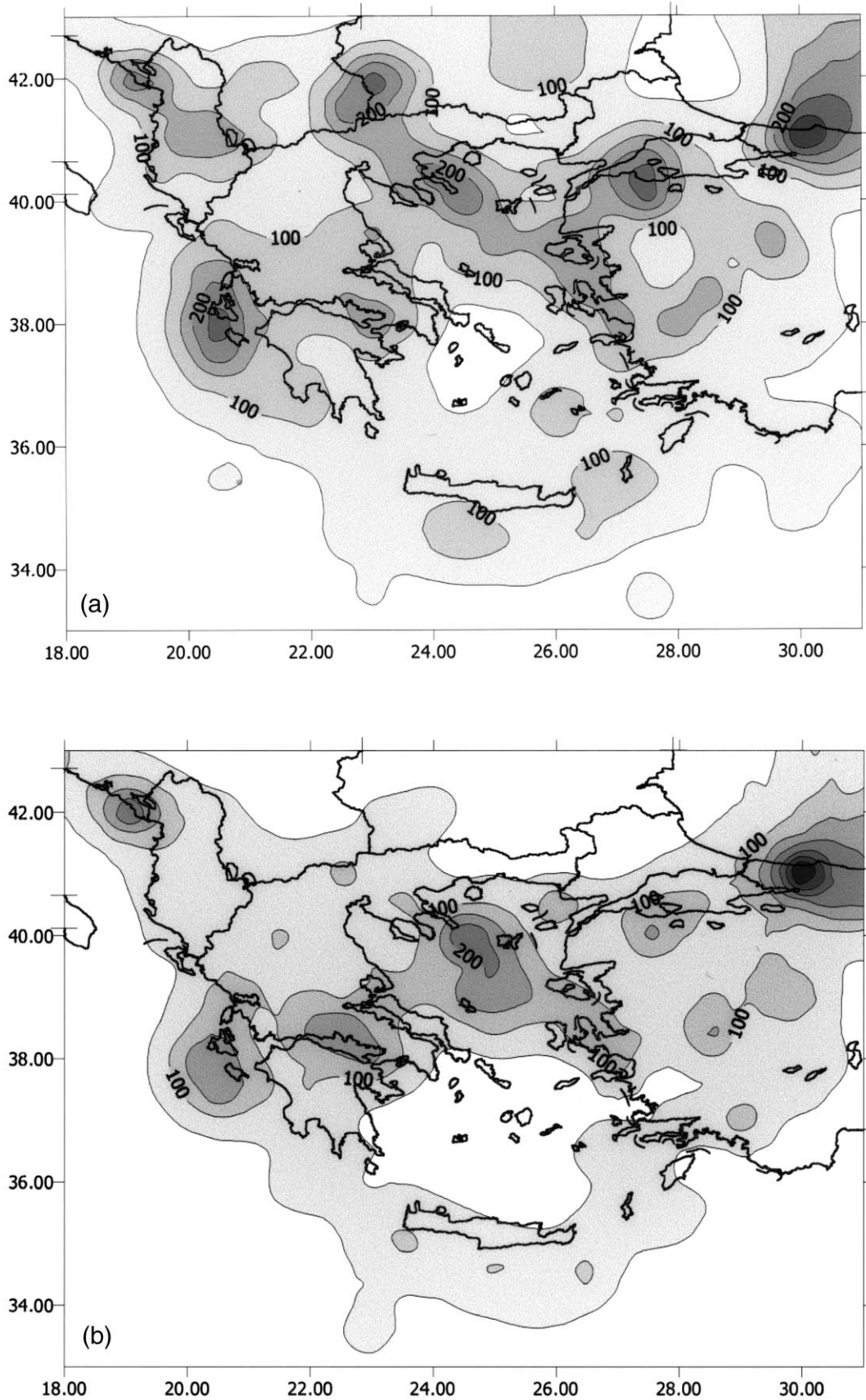
Fig. 3 (*continued*)

Fig. 4. Seismic hazard maps for Greece using the MB attenuation relationship, illustrating contours of expected maximum p.g.a. cm s^{-2} with 70% p.n.b.e. during 50-year: (a) using data 1900–1999 with $M_S \geq 5.5$; (b) using data 1964–1999 with $M_S \geq 4.0$.

The distributions or patterns of p.g.a. values resulting from analysis of modern data during 1964–1999 with magnitudes $M_S \geq 4.0$ in Fig. 3(d) are similar to the above analyses shown in Fig. 3(a). However, the level of the values in Fig. 3(d) is less than expected from the 100-year earthquake catalogue experience in Greece. This is simply because the time period for Fig. 3(d) is only 36 years which, irrespective of any view on the quality of modern data, is a little short for this study on maximum expected p.g.a. with 90% probability of not being exceeded in 50-year: whereas primary occurrences of seismicity, for example magnitude recurrence, might be extrapolated, it is difficult to extrapolate a secondary seismicity occurrence of p.g.a. over such a statistical term.

The second zone of note with high p.g.a. values in Fig. 3(a) is evident at the western on-shore end of the Northern Anatolia Fault—values reach in excess of 400 cm s^{-2}. Values further west in the Marmara Sea and parts of western Turkey and at Lesvos island are higher than 200 cm s^{-2}. In the western Marmara Sea, east of the Dardanelles, the p.g.a. values are generally over 300 cm s^{-2} and in some places over 350 cm s^{-2}. These values are larger than depicted in the 1985 map of Makropoulos and Burton [27] because the catalogue of earthquakes used here contains new large events in this area such as the catastrophic earthquakes of 1999 August 17 and November 12 near Izmit and Düzce [8,48].

The pattern of p.g.a. values obtained using the modern data during 1964–1999 (Fig. 3(d)) is again similar to the results using 1900–1999 (Fig. 3(a)), but on this occasion the high values at the western on-shore end of the Anatolian Fault are similar, presumably because both catalogue spans encompass the recent Izmit and Duzce earthquakes. However, the level of values for the western Marmara Sea and Lesvos are again smaller in Fig. 3(d) than in Fig. 3(a), presumably again attributable to the shorter 36-year catalogue span of the modern data. The NEAK places Lesvos island in Hazard Zone III in Fig. 1 (with p.g.a. value about 235 cm s^{-2}), indistinguishable from the results in Fig. 3(a).

The third zone with high p.g.a. values is the Chalkidiki Peninsula, south of Thessaloniki, extending northwestwards to the boundaries between Greece, Bulgaria and Macedonia. The p.g.a. values are in the range $200–300 \text{ cm s}^{-2}$ and even reach to the 350 cm s^{-2} contour in a small area of western Bulgaria. The NEAK map of Fig. 1 stops at the Greek border and otherwise places much of what is Greek territory in the Hazard Zone III (p.g.a. values about 235 cm s^{-2}). In view of the complexity of mapped p.g.a. variation in this area, and given that some p.g.a. values in Fig. 3(a) are higher than those for the NEAK Hazard Zone III, Fig. 3(a) provides a reference for comparison with the effective acceleration used in NEAK zones resulting from any future reevaluation of this region.

The patterns of p.g.a. values for the Chalkidiki Peninsula are depicted in Fig. 3(a) and (d), with values in Fig. 3(d)

being the smaller as usually expected. However, the region with the high p.g.a. values in the boundary area between Greece, Bulgaria and Macedonia that were seen in Fig. 3(a) can not be seen in Fig. 3(d). As a result this region with high p.g.a. values circa 300 cm s^{-2} becomes a blind seismic hazard zone in Fig. 3(d).

In addition to the above three zones, the area including the Gulf of Corinth and the Patras Gulf also has relatively high values (Fig. 3(a)). These values would typically be encompassed by a contour exceeding 150 cm s^{-2} (that could be extended to embrace Lamia, Volos, the Pagasitichos Gulf, and Larisa) but can reach over 200 cm s^{-2} in places, the latter contour in the Gulf of Corinth being on this occasion emphasized by Fig. 3(d) (presumably because of the Corinth 1981 earthquake sequence). A zone shape in central Greece spanning: the Patras Gulf, eastwards along the Gulf of Corinth, then northwards embracing Lamia, Volos and Larisa agrees with the NEAK zoning. However, the NEAK map places this entire area in its Hazard Zone III (p.g.a. values about 235 cm s^{-2}) whereas Fig. 3(a) has most of this area in the range $150–200 \text{ cm s}^{-2}$, the difficulty seems to be caused largely by the region exceeding 200 cm s^{-2} in the Gulf of Corinth itself. Invoking the progressively more onerous conditions expressed in Fig. 3(b) and (c), i.e. extending from the 475-year event through the 950-year to the 1900-year average return period event, does lead to values in excess of 200, even 250 cm s^{-2} for this zone.

It is also appropriate to delineate zones with low p.g.a. values using the evidence of Fig. 3. The first low zone, the largest in area, is in the Aegean Islands where much of the area has values below 100 cm s^{-2} and some is below 50 cm s^{-2} (Fig. 3(a)). The second low zone is located in the north-eastern part of Greece, between the Aegean shore line of Greece and the boundary between Greece and Bulgaria, where values are below 100 cm s^{-2}. The third low zone with values under 100 cm s^{-2} is the smallest and it is situated in the northern part of Greece. These zones are all to some extent compatible with the NEAK Hazard Zone I (p.g.a. value about 118 cm s^{-2}). The first and second low zones agree well with the extent of the NEAK zones. The third low zone, in the northern part of Greece, is smaller in Fig. 3(a) than in Fig. 1. Indeed, much of the NEAK zone for this area in Fig. 1 has values in the range $100–150 \text{ cm s}^{-2}$ in Fig. 3(a) or reaching 15%g (note that NEAK Zone II adopts 16%g). Theodulidis et al. [47] assessed seismic hazard of Kozani-Grevena which is in this third low zone. Their expected value of p.g.a. is about $150–200 \text{ cm s}^{-2}$ for a 475-year average return period; they also included data for the Kozani (1995 May 13, $6.6M_W$) earthquake in the region. There is a fourth low zone in Fig. 1 in north-eastern Greece, adjacent to the Bulgarian border and extending westwards as far as $\sim 23°E$. This is not discernible so far westwards in Fig. 3(a), nor is the low zone discernible in north-eastern Greece divisible in Fig. 3(a). The more onerous conditions expressed in the maps of Fig. 3(b) and (c) continue to

identify the first and second low zones in the Aegean Islands and in north-eastern Greece.

Large areas of central northern Greece and of the southern Peloponnisos show values below 150 cm s^{-2} in Fig. 3(a) and these are compatible with NEAK Hazard Zone II (p.g.a. value 16%g, or about 157 cm s^{-2}).

5.2. Seismic hazard evaluations and maps derived from the 'AM' model

Results obtained using the AM attenuation relationships in Eqs. (6b) and (6d) are shown in Fig. 5 which displays p.g.a. values with a 475-year average return period. Technically, Fig. 5 shows maximum p.g.a. values with a 90% probability of not being exceeded (p.n.b.e.) in the next 50-year, the calculations being based on earthquakes occurring during 1900–1999 with magnitude $M_S \geq 5.5$. Fig. 5(a) results from the AM attenuation relationship without depth control (Eq. (6b)) and Fig. 5(b) from the AM attenuation relationship with depth control (Eq. (6d)). Eqs. (6b) and (6d) were determined for earthquakes with magnitudes in the range $5.0 \leq M_S \leq 7.3$ (see Section 4) and so are entirely appropriate to the earthquake catalogue analyzed for 1900–1999. Values in Fig. 5(a) and (b) are 50-percentiles at rock sites.

Comparing results from the AM model without depth control in Fig. 5(a), with results based on the MB model in Fig. 3(a), demonstrates an obvious and expected similarity between the patterns of zones with relatively high or low p.g.a. values. The striking difference between Figs. 5(a) and 3(a) (or NEAK zones in Fig. 1) is that the level of the p.g.a. value in Fig. 5(a) is generally about 100 cm s^{-2} smaller than that in Fig. 3(a) or Fig. 1 (NEAK). The results based on the AM model with depth control shown in Fig. 5(b) are even smaller. The difference between these results and those based on the MB model or the NEAK zones is about 150 cm s^{-2}. These differences of level or scale in these seismic hazard maps suggest that use of the AM models in Greece may deviate significantly from the reality of seismicity in Greece.

5.3. Seismic hazard evaluations and maps derived from the 'TP' model

As discussed in Section 4, the TP model of Eq. (5) for rock sites [44] draws directly on 105 horizontal accelerogram recordings observed in Greece. The new TP model, NTP of Eq. (5a), is identified by Theodulidis (written communication) as being particularly appropriate, identifying stiff soil site characteristics as the main feature in its favour. Therefore the TP model and its variant provide a reasonable and Greece-specific model to apply to p.g.a. seismic hazard evaluation for Greece. Results for horizontal p.g.a. from the TP model are shown in Fig. 6, while the larger body of results is obtained from the NTP model preferred by Theodulidis and illustrated in Fig. 7(a)–(d) and Fig. 8.

Technically, Fig. 6 shows maximum p.g.a. values from the TP model with 90% p.n.b.e. in the next 50-year, the calculations drawing on the earthquake catalogue spanning 1900–1999 with magnitude $M_S \geq 5.5$. Fig. 7(a) which adopts the NTP model, is otherwise identical to Fig. 6, and may be compared directly with Fig. 6, Fig. 1 (NEAK zones) and Fig. 3(a) (MB model). Fig. 7(b) is the 200-year 90% p.n.b.e. NTP result using 1900–1999 earthquake data. Fig. 7(c) is like Fig. 7(a) except at 70% p.n.b.e. during 50-year. Fig. 7(d) is also like Fig. 7(a) except resulting from the earthquake catalogue spanning 1964–1999.

The emphasis in the following detailed discussion will draw on Fig. 7(a), that is the NTP model of the attenuation relationship used to produce p.g.a. results at the 50-percentile level with 90% p.n.b.e. during 50-year at stiff soil sites in Greece and calculated using the earthquake catalogue spanning 1900–1999 with magnitude $M_S \geq 5.5$. The vital comparative figures are: Fig. 1 (NEAK Zones), Fig. 3(a) (MB model), Fig. 6 (TP model) and Fig. 7(a) (NTP model).

The first zone through Levkas–Cephalonia–Zakinthos islands and Albania in the Hellenic Arc reaches higher values with the TP (Fig. 6) and the NTP models (Fig. 7(a)) than with the MB model (Fig. 1(a)). This area of the Hellenic Arc can be divided further into three sections. In the NW Section, Albania, the TP values are larger than 400 cm s^{-2} (Fig. 6) over a large area, NTP values (Fig. 7(a)) also exceed 400 cm s^{-2} but over a lesser area (Fig. 7(a)), while those for the MB model are about 200–250 cm s^{-2} (Fig. 1(a)). In the Main Section, Levkas–Cephalonia–Zakinthos islands, TP model values are larger than 400 cm s^{-2}, NTP model values just exceed 400 cm s^{-2} in a small area of Cephalonia, while MB model values only exceed 300 cm s^{-2}, albeit over a substantial area. In the further SE-Central Section of the Hellenic Arc, South of the Peloponnese-western Crete, the TP model values exceed 300 cm s^{-2}, NTP model values exceed 300 cm s^{-2} in parts of the area, but MB model values are usually only 100 + cm s^{-2}. The MB model values are considered to be too low in this section and inappropriate.

Levkas–Cephalonia–Zakinthos islands, coincide with NEAK Hazard Zone IV (36%$g \sim 353$ cm s^{-2}, NEAK, or 37%$g \sim 363$ cm s^{-2}, [34]). A p.g.a. value about 360 cm s^{-2} appears low compared with the above results based on TP and NTP models in parts of this zone. Fig. 6 of Slejko et al. [41, Fig. 6, p.1099] also suggests that the p.g.a. with 475-year average return period for Cephalonia is larger than 400 cm s^{-2}. On-the-other-hand, our values and NEAK's are lower than Slejko et al. for Corfu. A generality also emerges in that p.g.a. values are ordered TP > NTP > MB in our maps, consistent with simple expectations arising from illustrations of the attenuation relationships in Fig. 2.

The second zone is the western on-shore end of the Northern Anatolia Fault, where values are very high, and further west in the Marmara Sea and parts of western Turkey and at Lesvos island. At Lesvos Island the hierarchy of
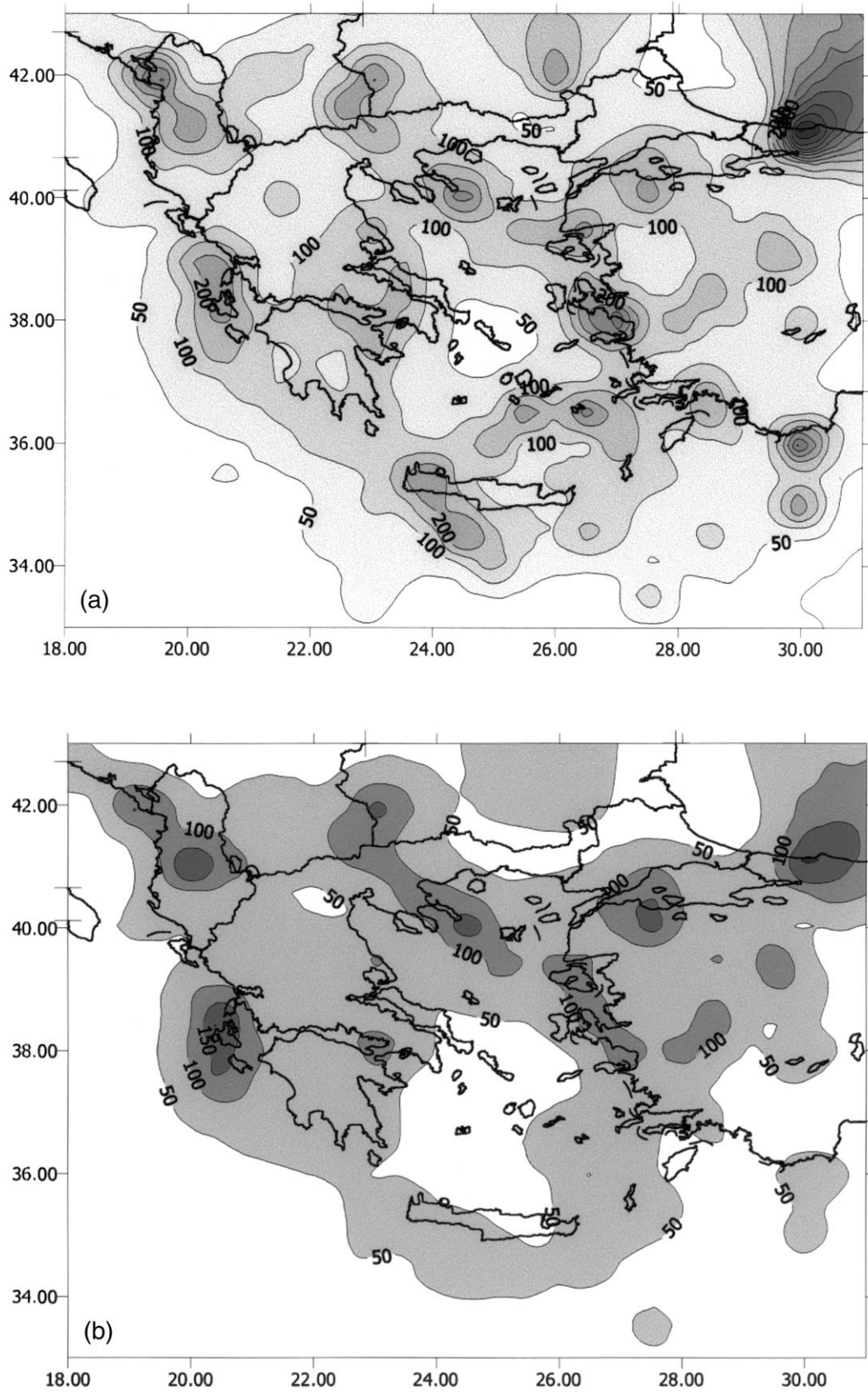
Fig. 5. Seismic hazard maps for Greece using the AM attenuation relationships. Contours are expected maximum p.g.a. cm s^{-2} with 90% p.n.b.e. during 50-year. Fifty-percentile values for rock sites using data 1900–1999 with $M_S \geq 5.5$ are shown, derived from the AM model: (a) without and; (b) with depth control.
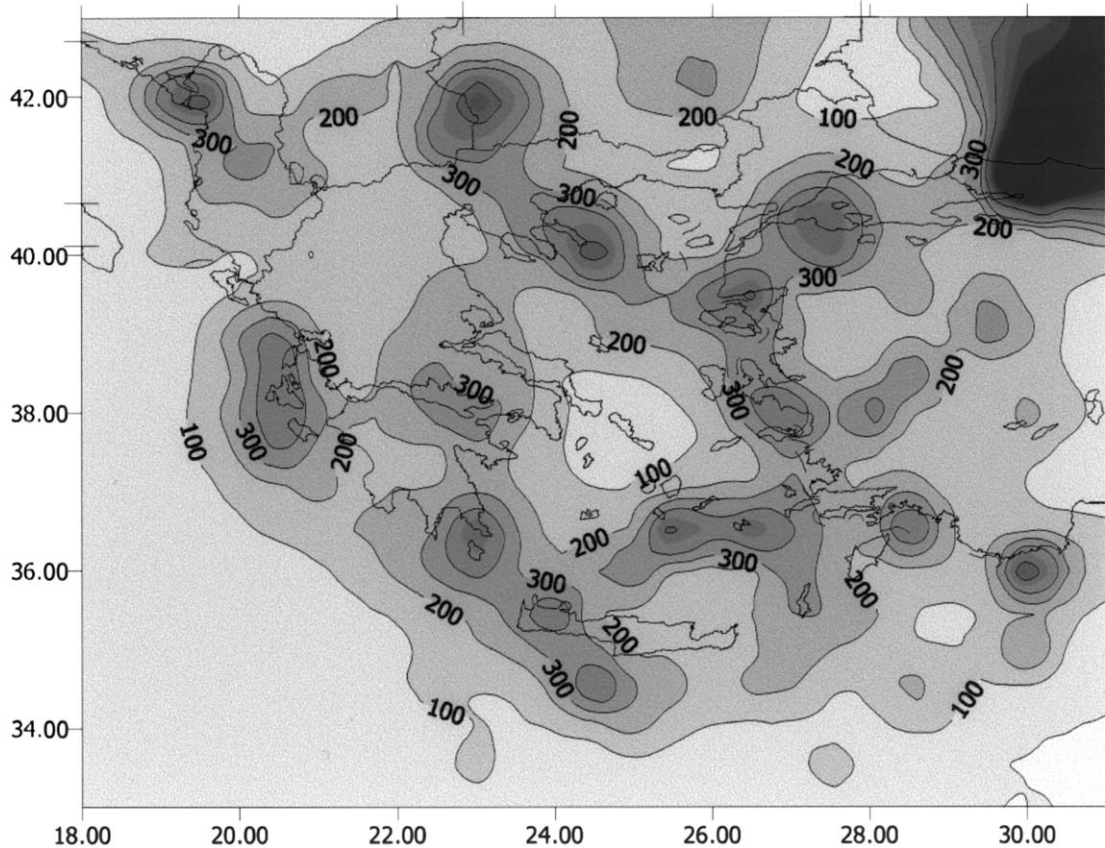
Fig. 6. Seismic hazard map for Greece using the TP attenuation relationship for rock sites. Contours are expected maximum p.g.a. cm s^{-2} with 90% p.n.b.e. during 50-year for 50-percentile values using data 1900–1999 with $M_S \geq 5.5$.

mapped p.g.a. values is: MB model ≥ 200 cm s^{-2}, NTP model ≥ 300 cm s^{-2}, and TP model ≥ 400 cm s^{-2}. The NTP model values extend to over 400 cm s^{-2} in north Lesvos. NEAK places Lesvos and the eastern-most Aegean in their Zone III ($24\%g \sim 235$ cm s^{-2}, NEAK, or $25\%g \sim 245$ cm s^{-2}, [34]); these values seem low even by the preferred NTP model (TP model would be higher) and Lesvos Island at least seems appropriate to higher Zone IV level values. Erdik et al. [17] also suggest values for this region in excess of 400 cm s^{-2}. However, it should be noted that the hazard contours in the northeast zone of our figures indicate unreasonably high seismic hazard in the offshore Black Sea. This is at the edge of our analysis. We have checked all earthquake records in this region in the database [13] used. The major event of 1999 (1999 August 17, 41.01°N 29.97°E, 7.8M_S) has epicentre extremely close to a grid point (41.00°N 30.00°E) used in the analysis. This will cause unreasonably high seismic hazard estimates in this local area because of the nature of the attenuation relations used in the seismic hazard evaluation. To solve this specific problem, we might choose different patterns of grid points and compare them to seek a reasonable evaluation. However, this paper essentially focuses on Greece proper. It is not intended herein to enlarge the north-eastern boundary of the working area which is at the edge of our objective area. Therefore a more reasonable evaluation for

this specific locality (the Black Sea Region) would require further detailed study.

The third zone is Chalkidiki Peninsula, south of Thessaloniki, extending northwestwards to the boundaries between Greece, Bulgaria and Macedonia. The TP model places this entire area in one zone with p.g.a. values in excess of 300 cm s^{-2} with large tracts in excess of 400 cm s^{-2}. NEAK shows an enclosed Zone III ($24\%g \sim 235$ cm s^{-2}) stopping in the northwest just short of the Macedonia border. NTP model places this entire zone with p.g.a. values in excess of 200 cm s^{-2} with substantial parts in excess of 300 cm s^{-2}, particularly around the Greece–Bulgaria–Macedonia borders. The preferred NTP results themselves suggest that parts of this zone require a higher level of attention, and the higher TP model values would only serve to underline this conclusion.

In the zone spanning the Gulf of Corinth and the Patras Gulf, where the MB model generally indicates $150+$ cm s^{-2}, the TP model indicates 200–$300+$ cm s^{-2}. Extending this zone to include Lamia, Volos, the Pagasitichos Gulf, and Larisa produces a zone entirely within one TP model contour at $200+$ cm s^{-2}, with the higher values centred on the Gulf of Corinth. NTP is compatible with this extended zone contained within a $200+$ cm s^{-2} contour, similar to the level and shape of the NEAK Zone III ($24\%g \sim 235$ cm s^{-2}, NEAK, or
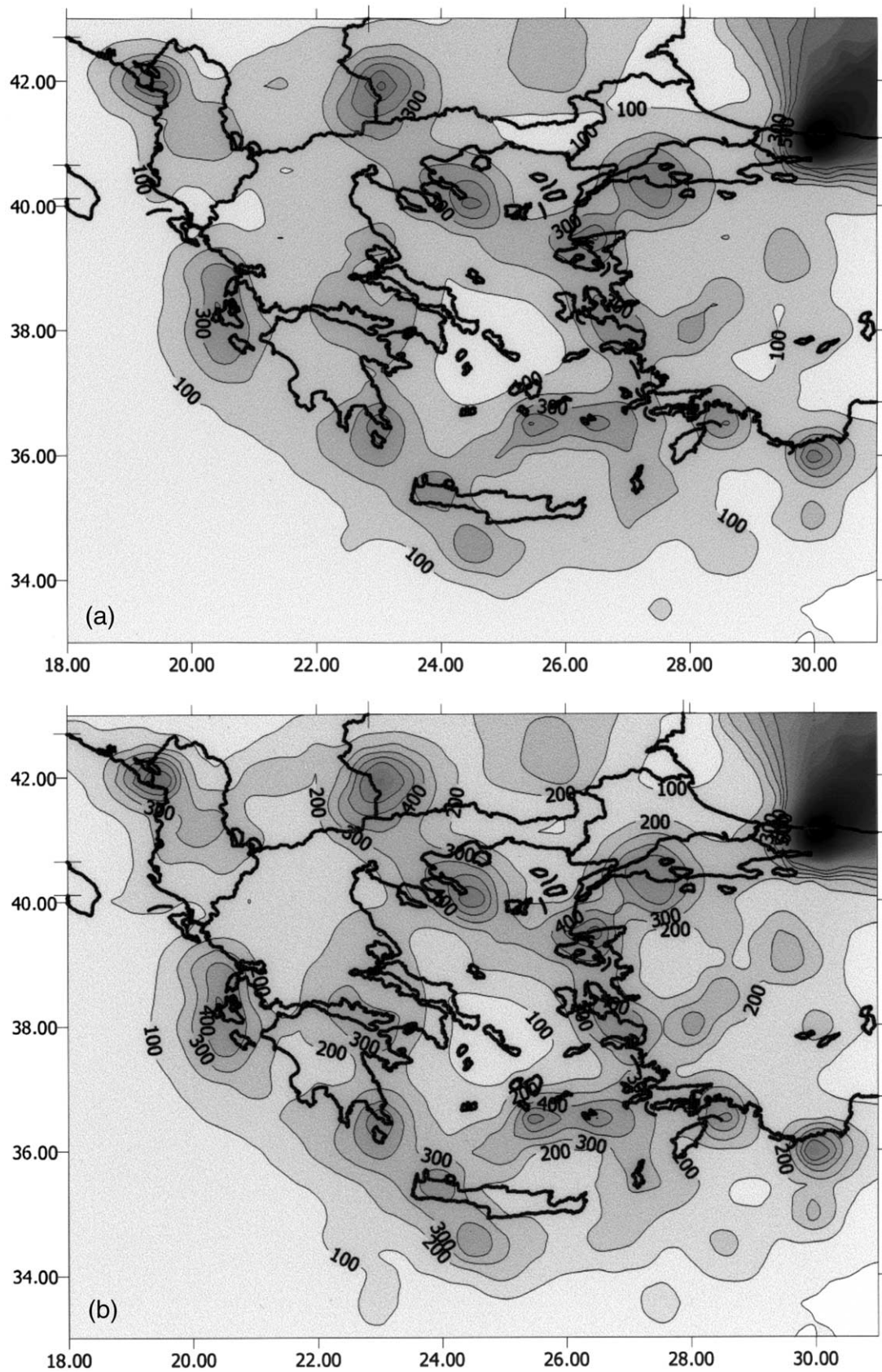
Fig. 7. Seismic hazard maps for Greece using the NTP attenuation relationship for stiff soil sites. Contours are expected maximum p.g.a. cm s^{-2} for 50-percentile values using data 1900–1999 with $M_S \geq 5.5$: (a) 90% p.n.b.e. during 50-year; (b) 90% p.n.b.e. during 200-year; (c) 70% p.n.b.e. during 50-year; and (d) 90% p.n.b.e. during 50-year using data 1964–1999.
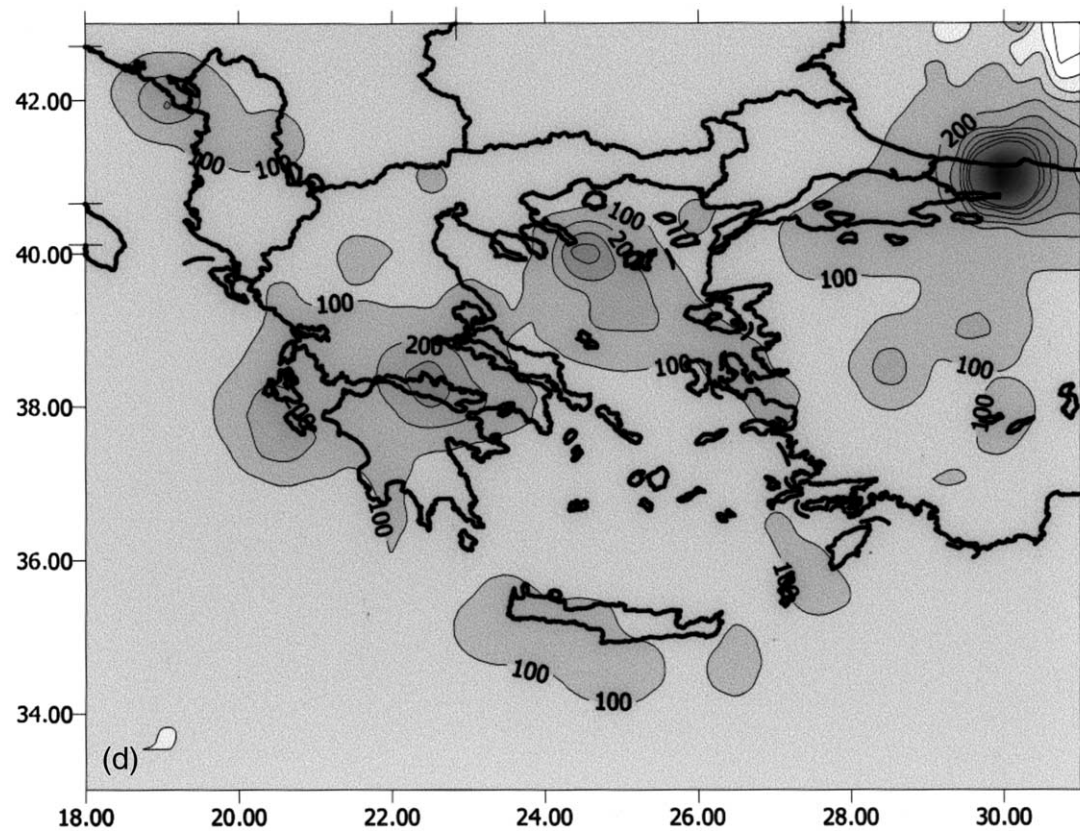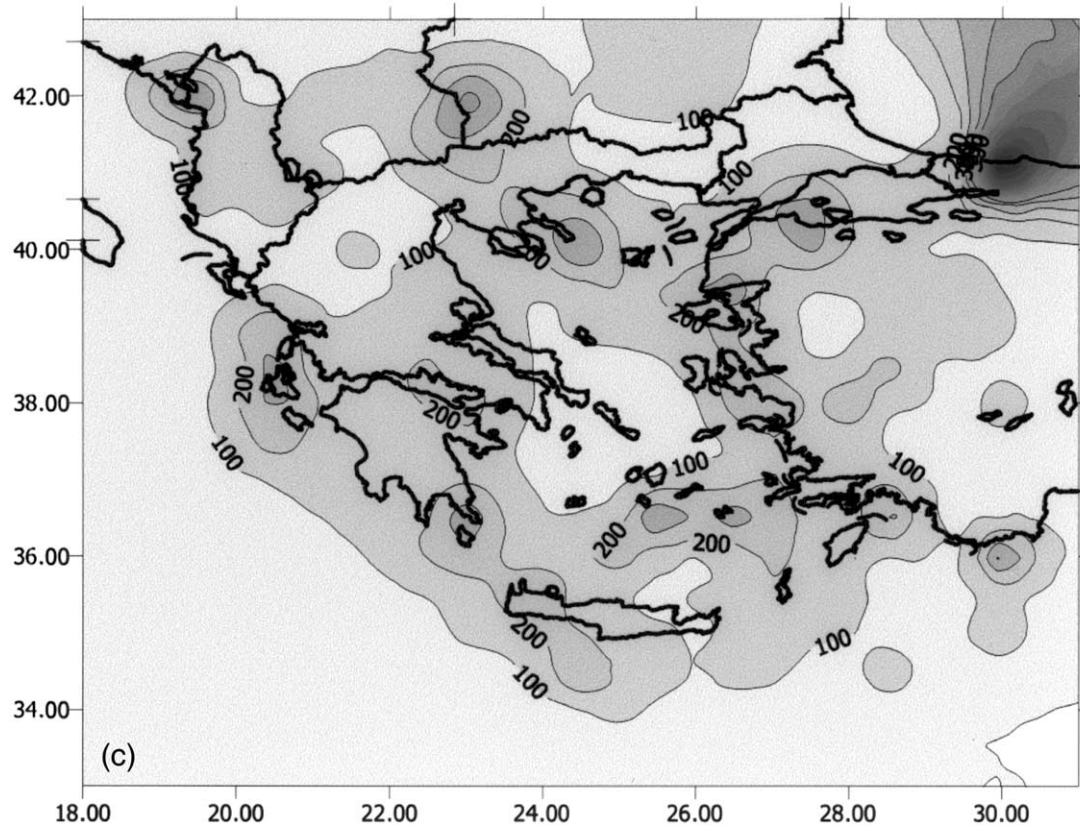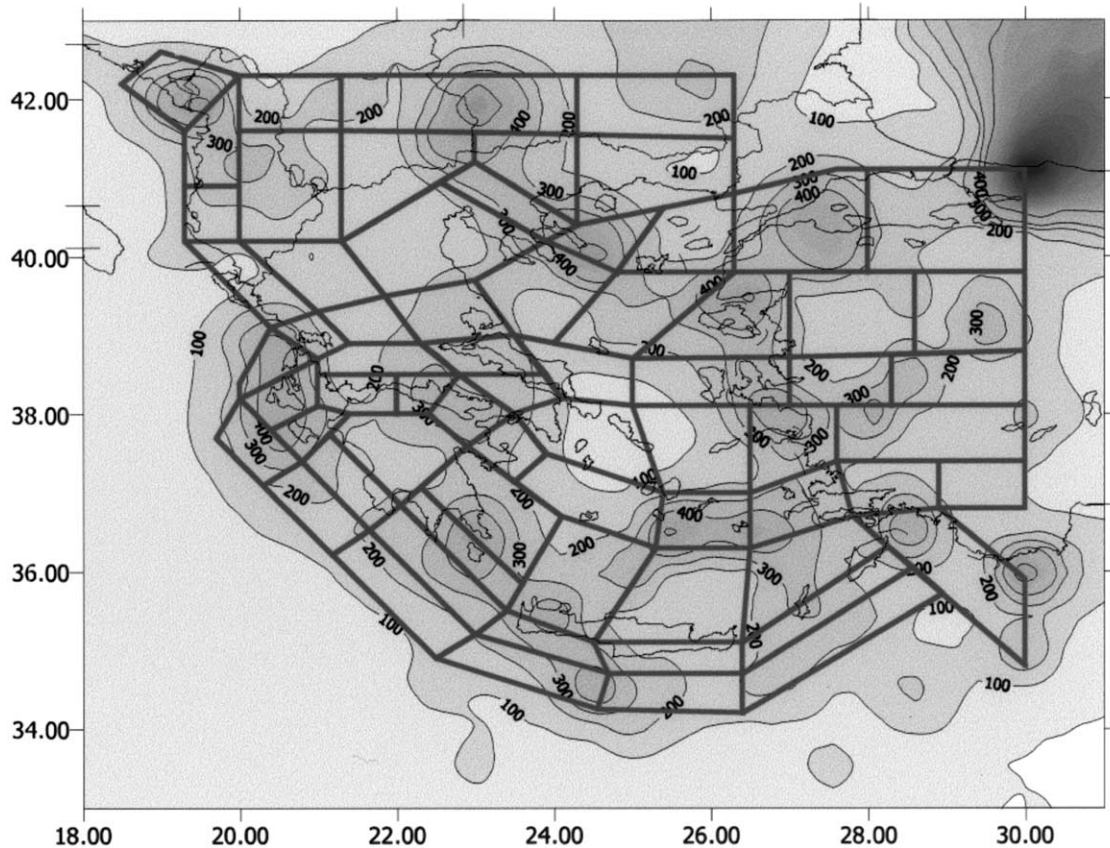
Fig. 7 (*continued*)

Fig. 8. Seismic hazard map for Greece using the NTP attenuation relationship for stiff soil sites with the 67 Papazachos and Papaioannou seismogenic source zones ([34]) superimposed. Contours are expected maximum p.g.a. cm s^{-2} with 90% p.n.b.e. during 50-year for 50-percentile values using data 1900–1999 with $M_S \geq 5.5$.

25%$g \sim 245$ cm s^{-2}, [34]). The more onerous condition of the 200-year 90% p.n.b.e. NTP model results in Fig. 7(b) fully endorse the shape and level of this extended zone.

It is useful to compare these high and moderate zones with those in the map of Erdik et al. [17, Fig. 5, p.1136] before proceeding to the low zones, bearing in mind that Erdik et al.'s map addresses a substantially larger area, viz. circa 35–43°N 19–47°E.

In the map of Erdik et al. there is a NE–SW trending zone stretching from Volos to Levkas with high p.g.a. values (0.5–0.6 g). Our map (Fig. 7(a)) corresponding to this distribution for high p.g.a. values shows two separated areas: the larger zone being Levkas–Cephalonia–Zakinthos islands (≥ 300 cm s^{-2}), the smaller being associated with Volos (≥ 200 cm s^{-2}). Our expected p.g.a. values are typically smaller than in Erdik et al.'s mapped zone, and the total area for these two sections combined in our map is also much smaller. To reach 500 cm s^{-2} in Cephallonia our analysis must extend to 200-years at the 90% level (Fig. 7(b)).

The second high p.g.a. distribution (0.5–0.6 g) in Erdik et al.'s map is in the eastern Chalkidiki Peninsula zone. The range west to east through the Chalkidiki Peninsula in both studies is 200 cm s^{-2} to over 500 cm s^{-2}. Corresponding to this distribution, the expected p.g.a. values for the eastern Chalkidiki Peninsula from our results are generally larger than 300 cm s^{-2}. There is also very high expected p.g.a. in excess of 500 cm s^{-2} contoured in the Chalkidiki Peninsula from our results, at the easternmost tip of the Peninsula, but its area is much smaller than that of Erdik et al.'s study. In addition, our spatial definition of this zone extends north-westwards towards the boundary between Greece, Bulgaria and Macedonia. Extending to the 200-year analysis at the 90% level (Fig. 7(b)) increases our value of p.g.a. to over 600 cm s^{-2} at the easternmost tip of the Peninsula.

Except for the above two high p.g.a. zonal distributions, Erdik et al. indicate that the values for the remainder of Greece are in the range 0.4–0.5 g, although they do not research this territory in detail as a primary target. Our values for the remainder of Greece, based on the NTP model (Fig. 7(a)) are usually in the range 100–200 cm s^{-2} (sometimes slightly higher), generally compatible with NEAK, and less than in the map of Erdik et al., with the corresponding area shrinking slightly when extended to 200-year analysis. Additionally, there are detailed divisions in Fig. 7(a), among them, the Gulf of Corinth is an important high value area (≥ 200 cm s^{-2}) that increases to over 300 cm s^{-2} when the 200-year analysis at the 90% level is considered (Fig. 7(b)).

The above comparison shows that the main expected ranges (high and lower) of p.g.a. distributions from Erdik et al. are not greatly different from ours. As we know, Erdik et al.'s study was fundamentally different, being based on tectonic zonations whereas we adopt zone-free analysis. Also the attenuation models and database for Erdik et al. are different from ours. Therefore it is easy to understand that results will differ. The more important difference is that Erdik et al.'s study emphasises Turkey whilst ours focuses on Greece—therefore different underlying decisions have also been taken. Amongst these is recognition that the attenuation laws of Boore et al. [10], Campbell [14] and Sadigh et al. [38], used by Erdik et al., do not lean towards analysis of European strong motion data. Boore et al. in particular includes strike-slip earthquake strong motion—such considerations are directly pertinent to Anatolia in Turkey, whereas Greece does not have a similar tectonic feature. The NTP model used herein came directly from the Greek strong motion data and thus represents the most advanced study for attenuation relations applicable to Greece. Our results can more objectively provide a more detailed assessment of earthquake hazard for Greece.

Conclusions based on the NTP model for the low zones are similar to, but not identical with, those obtained from the MB model. The development from MB to NTP low zones must be accompanied by: (1) a small increase in p.g.a. for similar zone area, or (2) zone area must shrink slightly for an NTP low zone if the p.g.a. value is maintained at the MB level, or (3) a combination of (1) and (2). The first low zone remains as the most substantial area in the Aegean Islands with p.g.a. values below $100 \, \mathrm{cm \, s^{-2}}$ over a significant area. The second low zone in the north-eastern part of Greece, between the Aegean shore line of Greece and the boundary between Greece and Bulgaria, also has substantial area below $100 \, \mathrm{cm \, s^{-2}}$ (this zone would shrink to become a small area if the TP model results were preferred). Note that division of the low zone in northeastern Greece apparent in the NEAK map (adjacent to the Bulgarian border and extending westwards as far as $\sim 23°$E) is not discernible in the NTP model results mapped in Fig. 7(a).

The third low zone with values under $100 \, \mathrm{cm \, s^{-2}}$, which is situated in the northern part of Greece, becomes separated into one sub-zone east of Albania and a second sub-zone in southern Albania in Fig. 7(a). These sub-zones become diminutively small when the 200-year 90% p.n.b.e. condition of Fig. 7(b) is inspected, particularly so for the sub-zone in northwest Greece. It would be appropriate to adopt values in excess of $100 \, \mathrm{cm \, s^{-2}}$ throughout this area, compatible with the conclusions of Theodulidis et al. [47]. The weight of evidence from MB maps in Figs 3(a)–(c) and the preferred NTP maps of Fig. 7(a) and (b) underlines identification of the first and second low zones in the Aegean Islands and in north-eastern Greece.

6. Conclusions

Six reasons were put forward in the Introduction for pursuing these studies. Briefly, these are

1. An additional 21 years of high quality earthquake catalogue data has accumulated since Makropoulos and Burton [27] produced maps of p.g.a. seismic hazard in Greece. It is pertinent to examine the impact of these new data on seismic hazard estimates.
2. There has been an accumulation of earthquake strong motion data in Europe since 1985, some of it obtained in situ in Greece, with commensurate improvement in our knowledge base for appropriate attenuation relationships.
3. There is need to assess expected levels of ground motion at the Revithoussa liquid natural gas hydrocarbon storage site, adjacent to Athens, as the focus for an earthquake early-warning demonstration shield.
4. GSHAP published the first global map of seismic hazard in 1999 but with the Greek territory forming parts of two analyses directed at Italy and Turkey, respectively; it is therefore appropriate to focus analysis on Greece.
5. The NEAK has been applied since 1996 and is based on the Seismic Hazard Zoning map shown in Fig. 1. Comparisons between NEAK and our new results help to form an ongoing basis for zoning and related safety improvements.
6. Papaioannou and Papazachos [34] present comprehensive seismic hazard results for Greece, dependent on defining 67 Euclidean seismogenic sources or zones. The studies in the present paper are zone-free. Our results are shown underlying the Papaioannou and Papazachos zones in Fig. 8.

Conclusions are

- the adopted zone-free methodology is successful.

The increased catalogue length, 21 years of high quality modern data, alone leads to changes in the previous seismic hazard results obtained [27], and it is found that

- these changes are usually encouragingly small and amount to perturbations of about 10% to the 50-year 70% p.n.b.e. value of p.g.a. at six cities in Greece (from inspection of Table 1).
- two cities only, Athens and Corinth, show an increased hazard whereas Heraklion, Patras, Rodhos and Thessaloniki show a small decrease.
- use of the modern earthquake period alone i.e. 1964–1999 allows analysis down to a lower magnitude threshold (4.0 rather than $5.5M_S$), however, p.g.a. results that ensue are consistently lower when derived from the period 1964–1999 than from 1900–1999.

The accumulation of earthquake strong motion data in Europe since 1985 has lead to new attenuation relationships, some of which concentrate on the Greek strong motion database. The MB model originally used by Makropoulos and Burton [27] was used as a benchmark to consider change. The new attenuation relationships are drawn from the several AM models (see e.g. [3]) and the TP models [44] with its stiff soil site variant (Theodulidis, pers. comm.: NTP model herein). The pattern of site-specific results for six cities in Greece (Tables 2 and 3) is, unsurprisingly, entirely systematic. The pattern of the calculated level of hazard values at each city follows: TP (rock sites) > NTP (TP corrected stiff soil sites) > MB (bench mark) ≅ AM1 (rock sites, without depth control) > AM2 (rock sites, with depth control). Progress in the TP models towards an attenuation relationship designed explicitly for Greek seismicity and, what is subsequently seen to be a degree of accord with the level of p.g.a. seismic zones expressed as Greek experience in the NEAK Seismic Hazard Zones, leads to adoption of the TP (rock site) and particularly to the NTP (stiff soil site) for production of isoacceleration maps.

The patterns of spatial distribution of p.g.a. in the isoacceleration maps derived from all of the attenuation relationships are all broadly consistent with the results of Makropoulos and Burton [27] and the NEAK, although the levels of the hazard differ. The new results from the Theodulidis and Papazachos model for stiff soil sites (Fig. 7(a) and (b)) suggest for the high zones that

- the first zone in Levkas–Cephalonia–Zakinthos islands should increase to just over 400 cm s^{-2} (also see Slejko et al. [41]).
- the second zone including west in the Marmara Sea and parts of western Turkey and at Lesvos island should consider the range 300–400 cm^{-2} at Lesvos Island and even higher values in parts of Marmara, etc. (also see Erdik et al. [17]).
- the third zone spanning Chalkidiki Peninsula, south of Thessaloniki, extending northwestwards to the boundaries between Greece, Bulgaria and Macedonia requires considerable attention to define both its shape and level: substantial tracts should be in excess of 300 cm s^{-2}.

It is concluded for the low zones that

- the large zone delineated in the Aegean Islands and the smaller zone in northeastern Greece should remain, the latter as one contiguous zone rather than two.
- the zone east of Albania in northern Greece is unsustainable (also see [47]).

In general

- extension to the more onerous condition of the 200-year 90% p.n.b.e. isoacceleration map (Fig. 7(b)) reinforces the need to increase hazard-zoning p.g.a. levels in some areas, even in some relatively high zones like Lesvos Island, and only to accept the two regions of relatively low seismic hazard.

Acknowledgements

References

[1] Ahorner L, Rosenhauer W. Probability distribution of earthquake accelerations for the sites in Western Germany. Proceedings of the Fifth European Conference Earthquake Engineering, Istanbul; 1975.

[2] Ambraseys NN. The prediction of earthquake peak ground acceleration in Europe. Earthquake Engng Struct Dyn 1995;24: 467–90.

[3] Ambraseys NN. Measurement of strong ground motion in Europe (MASGE). In: Ghazi A, Yeroyanni M, editors. Seismic Risk in the European Union. Proceedings of the review meetings in Brussels 2–3 and 23–24 May 1996, ECSC-EC-EAEC Brussels, Luxembourg, vol. 1.; 1997. p. 195–217.

[4] Ambraseys NN, Simpson KA, Bommer JJ. Prediction of horizontal response spectra in Europe. Earthquake Engng Struct Dyn 1996;25: 371–400.

[5] Ambraseys NN, Simpson KA. Prediction of vertical response spectra in Europe. Earthquake Engng Struct Dyn 1996;25:401–12.

[6] Ambraseys N, Smit P, Beradi R, Rinalds D, Cotton F, Berge-Thierry C. European strong-motion database documentation, European Council. Environment and Climate Research Programme, (CD-ROM); 2000.

[7] Baba AB, Papadimiriou EE, Papazachos BC, Papaioannou CA, Karakostas BG. Unified local magnitude scale for earthquakes of south Balkan area. Pure Appl Geophys 2000;157:765–83.

[8] Barka A. The 17 August Izmit earthquake. Science 1999;285:1858–9.

[9] Bath M. Seismicity of the Tanzania region. Tectonophysics 1975;27: 353–79.

[10] Boore DM, Joyner WB, Fumal TE. Equations for estimating horizontal response spectra and peak acceleration from western North American earthquakes: a summary of recent work. Seismol Res Lett 1997;68:128–53.

[11] Burton PW. Seismic risk in Southern Europe through to India examined using Gumbel's third distribution of extreme values. Geophys J R Astr Soc 1979;59:249–80.

[12] Burton PW, McGonigle RW, Makropoulos KC, Ucer SB. Seismic risk in Turkey, the Aegean, and the eastern Mediterranean: the occurrence of large magnitude earthquakes. Geophys J R Astr Soc 1984;78: 475–506.

[13] Burton PW, Xu Y, Qin C, Tselentis G-A, Sokos EA. Catalogue of seismicity in Greece and the adjacent areas for the twentieth century; Tectonophysics 2002 (in press).

[14] Campbell KW. Empirical near-source attenuation relationships for horizontal and vertical components of peak ground acceleration, peak ground velocity, and pseudo-absolute acceleration response spectra. Seismol Res Lett 1997;68:154–79.

[15] Donovan NC. A statistical evaluation of strong motion data including the February 9, 1971 San Fernando earthquake. Proceedings of the Fifth World Conference on Earthquake Engineering, Rome; 1973.

[16] Engdahl ER, Hilst RVD, Buland R. Global teleseismic earthquake relocation with improved travel time and procedure for depth determination. Bull Seismol Soc Am 1998;88:722–43.

[17] Erdik M, Biro YA, Onur T, Sesatyan K, Birgoren G. Assessment of earthquake hazard in Turkey and neighbouring regions. Ann Geofis 1999;42:1125–38.

[18] Galanopoulos AG, Delibasis N. Map of maximum observed intensities in Greece (period 1800–1970), University of Athens; 1972.

[19] Giardini D, editor. The global seismic hazard assessment program (GSHAP) 1992–1999, vol. 42.; 1999.

[20] Gumbel EJ. Statistics of extremes. New York: Columbia University Press; 1966. 375 pp.

[21] Hamdache M. Seismic hazard estimation in northern Algeria. Nat Hazards 1998;18:119–44.

[22] ITSAK Strong-motion recording bulletins of the ITSAK's Network (period 1960–1994). Report ITSAK:97-01; 1997.

[23] Kalogeras IS, Stavrakakis GN. Analysis of Greek accelerograms recorded at stations of NOA's network, time period 1990–1994. National Observatory of Athens, Geodynamic Institute, Publication No. 5, Athens; 1995.

[24] Katayama T. Statistical analysis of peak acelerations of recorded earthquake ground motions. Seisan-Kenkyu 1974;26(1):18–20.

[25] Makropoulos KC, Burton PW. A catalogue of seismicity in Greece and adjacent areas. Geophys J R Astr Soc 1981;65:741–62.

[26] Makropoulos KC, Burton PW. Seismic hazard in Greece. I. Magnitude recurrence. Tectonophysics 1985;117:205–57.

[27] Makropoulos KC, Burton PW. Seismic hazard in Greece. II. Ground acceleration. Tectonophysics 1985;117:259–94.

[28] Makropoulos KC, Drakopoulos JK, Latousakis JB. A revised and extended earthquake catalogue for Greece since 1900. Geophys J Int Res Note 1989;98:391–4.

[29] Makropoulos K, Voulgaris N, Likiardopoulos A. A multi-methodological approach to seismic hazard assessment. An application for Athens (Greece). Proceedings of the XXII Gen. Ass. ESC. Barcelona; 1990. p. 585–91.

[30] Margaris VN. Azimuthal dependence of the seismic waves and its influence on the seismic hazard assessment in the area of Greece. PhD Thesis, Thessaloniki University; 1994. p. 324.

[31] Margaris BN, Papazachos CB. Moment-magnitude relations based on strong-motion records in Greece. Bull Seismol Soc Am 1999;89: 442–55.

[32] Musson RMW. Determination of design earthquakes in seismic hazard analysis through Monte Carlo simulation. J Earthquake Engng 1999;3:463–74.

[33] Orphal DL, Lahoud JA. Prediction of peak ground motion from earthquakes. Bull Seismol Soc Am 1974;64:1563–74.

[34] Papaioannou ChA, Papazachos BC. Time-independent and time-dependent seismic hazard in Greece based on seismogenic source. Bull Seismol Soc Am 2000;90:22–33.

[35] Papaioannou ChA. Attenuation of seismic intensities and seismic hazard in the area of Greece. PhD Thesis, Thessaloniki University; 1984. p. 200.

[36] Papazachos B, Papazachou C. The earthquakes of Greece. Thessaloniki: P. Ziti and Co; 1997. 304 pp.

[37] Pérez O. Revised world seismicity catalog (1950–1997) for strong ($M_S \geq 6$) shallow ($h \leq 70$ km) earthquakes. Bull Seismol Soc Am 1999;89:335–41.

[38] Sadigh K, Chang C-Y, Egan JA, Makdisi F, Youngs RR. Attenuation relationships for shallow crustal earthquakes based on California strong motion data. Seismol Res Lett 1997;68:180–9.

[39] Shah HC, Movassate M. Seismic risk analysis—California state water project. Proceedings of the Fifth European Conference on Earthquake Engineering, Istanbul; 1975.

[40] Schenkova Z, Karnik V. The probability of occurrence of largest earthquakes in the European area—part II. Pure Appl Geophys 1970; 80:152–61.

[41] Slejko D, Camassi R, Cecic I, Herak D, Herak M, Kociu S, Kouskouna V, Lapajne L, Makropoulos K, Meletti C, Muco B, Papaioannou C, Peruzza L, Rebez A, Scandone P, Sulstarova E, Voulgaris N, Zivcic M, Zupancic P. Seismic hazard assessment for Adria. Ann Geofis 1999;42:1085–107.

[42] Spudich P, Fletcher JB, Hellweg M, Boatwright J, Sullivan C, Joyner WB, Hanks TC, Boore DM, McGarr A, Baker LM, Lindh AG. SEA96—a new predictive relation for earthquake ground motions in extensional tectonic regimes. Seismol Res Lett 1997;68:190–8.

[43] Theodulidis NP. Contribution to study of strong motion in Greece. PhD Thesis, Thessaloniki University; 1991.

[44] Theodulidis NP, Papazachos BC. Dependence of strong ground motion on magnitude–distance, site geology and macroseismic intensity for shallow earthquakes in Greece: I, peak horizontal acceleration, velocity and displacement. Soil Dyn Earthquake Engng 1992;11:387–402.

[45] Theodulidis NP, Papazachos BC. Dependence of strong ground motion on magnitude–distance, site geology and macroseismic intensity for shallow earthquakes in Greece: II, horizontal pseudovelocity. Soil Dyn Earthquake Engng 1994;13:317–43.

[46] Theodulidis NP, Bard P-Y. Strong ground motion simulating of large earthquakes. Proc 10th Eur Conf Earthquake Engng 1995;1: 269–74.

[47] Theodulidis N, Lekidis V, Margaris B, Papazachos C, Papaioannou Ch, Dimitriu P. Seismic hazard assessment and design spectra for the Kozani–Grevena region (Greece) after the earthquake of May 13, 1995. J Geodyn 1998;26:375–91.

[48] Toksöz MN, Reilinger RE, Doll CG, Barka AA, Yalcin N. Izmit (Turkey) earthquake of 17 August. Seismol Res Lett 1999;70:669–79.

[49] Trifunac MD. Preliminary analysis of the peaks of strong earthquake ground motion—dependence of peaks on earthquake magnitude, epicentral distance, and recording site conditions. Bull Seismol Soc Am 1976;66:189–219.

[50] Tsapanos TM, Burton PW. Seismic hazard evaluation for specific seismic regions of the world. Tectonophysics 1991;194:153–69.

[51] Tselentis G-A, Melis NS, Sokos E. The Patras (July 14, 1993; $M_S = 5.4$) earthquake sequence. In: Proc. VIIth Congress Greek Geological Society, May, Thessaloniki. Bull. Geol. Soc. Greece 1994; XX:159–65.

[52] Yegulalp TM, Kuo JT. Statistical prediction of the occurrence of maximum magnitude earthquakes. Bull Seismol Soc Am 1974;64: 393–414.